Monocotyledonous plants graft at the embryonic root-shoot interface

Gregory Reeves[1,2], Anoop Tripathi[1], Pallavi Singh[1], Maximillian R. W. Jones[1], Amrit K. Nanda[3], Constance Musseau[3], Melanie Craze[2], Sarah Bowden[2], Joseph F. Walker[4], Alison R. Bentley[2,5], Charles W. Melnyk[3], Julian M. Hibberd[1*]

[1] University of Cambridge, Department of Plant Sciences, Downing Street, Cambridge, CB2 3EA, United Kingdom

[2] NIAB, 93 Lawrence Weaver Road, Cambridge, CB3 0LE, United Kingdom

[3] Swedish University of Agricultural Sciences, Department of Plant Biology, 756 51 Uppsala, Sweden

[4] Department of Biological Sciences, University of Illinois at Chicago, Chicago, IL, 60607 United States of America

[5] Present address: International Wheat and Maize Improvement Center (CIMMYT), El Batan, Mexico

* For correspondence: jmh65@cam.ac.uk

One sentence summary: Embryogenic tissues allow grafting within and between different species of monocotyledons.

Keywords: grafting, monocot, grasses, cereals, mesocotyl, vascular connection, wheat, rice, rootstock, scion, transcriptome

Grafting is possible in both animals and plants. Whilst in animals the process requires surgery and is often associated with rejection of non-self, in plants grafting is widespread, and has been used since antiquity for crop improvement[1]. However, in the monocotyledons, which represent the second largest group of terrestrial plants including many staple crops, the absence of vascular cambium is thought to preclude grafting[2]. Here, we show that the embryonic hypocotyl allows intra- and inter-specific grafting in all three monocotyledon groups: the Commelinids, Lilioids, and Alismatids. Functional graft unions were demonstrated through histology, application of exogenous fluorescent dyes, complementation assays for movement of endogenous hormones, and growth of plants to maturity. Expression profiling identified genes that unify the molecular response associated with grafting in monocotyledons and dicotyledons, but also gene families not previously associated with tissue union. Fusion of susceptible wheat scions to oat rootstocks conferred resistance to the soil-borne pathogen *Gaeumannomyces graminis*. Collectively, these data overturn the consensus that monocotyledons cannot form graft unions, and identify the hypocotyl (mesocotyl in grasses) as a meristematic tissue allowing this process. We conclude that graft compatibility is a shared ability among seed-bearing plants.

Grafting genetically distinct root and shoot tissues allows the introduction of traits ranging from shoot dwarfing to pest and disease resistance[1]. However, this ancient and widespread agricultural practice has not been applied to the monocotyledons that represent more than one fifth of the estimated 350,699 land plant species[3]. Monocotyledons are defined by one seed leaf (cotyledon) and many are crops cultivated at enormous scale. The last common ancestor of this clade is theorized to have lost grafting ability[2]. An absence of vascular cambium in monocotyledons—the meristematic tissue giving rise to secondary growth in dicotyledons and gymnosperms, and a scattered arrangement of vascular bundles are thought to cause this graft

failure (Supplementary Note 1). Thus, despite historical reports with low success rates (Supplementary Note 2)[4–6], grafting monocotyledons has never been routinely adopted in either discovery science or agriculture[7].

Discovery of grafting method

We investigated various approaches to better understand causes of graft incompatibility in monocotyledons and tested the hypothesis that undifferentiated tissues can graft. Surprisingly, this led us to identify a simple method allowing thousands of monocotyledons to be fused (Supplementary Table 1). First, we hypothesized that fusion of undifferentiated or embryogenic tissues allows the formation of graft-unions in grasses. Although numerous attempts with embryogenic callus failed (Extended Data Fig. 1a-d) we discovered that if the shoot (plumule) from an immature embryo of a wheat (*Triticum aestivum*) seed was replaced with analogous material from another seed, vestigial graft-like plants developed (Extended Data Fig. 1e). When mature embryos were used, grafts that resembled non-grafted plants were obtained (Fig. 1a, Extended Data Fig. 2a-f, and Video 1). A transgenic pUBIQUITIN::β-GLUCURONIDASE (GUS) wheat line was used to show that genetically distinct plants could be grafted and grown to maturity (Fig. 1b-e, Extended Data Fig. 2g-k). These intra-specific grafts regenerated normal unions delineated by the GUS marker. Elongated cells resembling callus (Fig. 1c, Extended Data Fig. 2h) and vascular strands connecting scion and root detectable (Fig. 1e, Extended Data Fig. 2j). Consistent with work on *Arabidopsis thaliana*[8], the fluorescent dye carboxyfluorescein diacetate (CFDA) transversed the graft junction. When applied to the scion CFDA was detected in the vascular cylinder of the rootstock within two hours (Fig. 1f, Extended Data Fig. 2l-o, t-v) and when applied to the rootstock CFDA was detected in the vasculature of the scion (Fig. 1f, Extended Data Fig. 2p-s, w-y). This is consistent with functional phloem and xylem connections across the graft junction. In all cases,

74 the graft union formed at the hypocotyl (known as the mesocotyl in grasses), which separates
75 the embryo's plumule and radicle. The efficiency of grafting wheat was highest when the
76 plumule was excised and replaced in the same seed (79 %, n = 78, Supplementary Table 1).
77 But, different hexaploid wheat genotypes also fused successfully (31 %, n = 345, Extended
78 Data Fig. 2k).
79
80 **Functional graft unions**
81 Grafting was also achieved in rice (*Oryza sativa*) (Fig. 1g) and longitudinal sections
82 indicated vascular continuity between root and shoot (Fig. 1h, Extended Data Fig. 3a-d). Graft
83 unions established in seven days (Fig. 1l). In the first three days, cells of the shoot and root
84 were often spatially separated, but from three to five days the gap between scion and rootstock
85 narrowed, and by day seven vascular differentiation was evident (Fig. 1j). Cells on both sides
86 of the graft interface elongated but those in the scion responded sooner and to a greater extent
87 (Fig. 1k). A reduction in cell length indicative of cell division in the scion was detected seven
88 days after grafting.
89 CFDA transversed the graft junction in under two hours (Fig. 1l, Extended Data Fig. 3e-t).
90 The speed of CFDA movement across the graft junction and its fluorescence being limited to
91 vascular tissues in both wheat and rice are compatible with vascular transport and incompatible
92 with diffusion. As with dicotyledon grafting[16], and indicating that phloem connections likely
93 form more quickly, CFDA movement from shoot-to-root was detected sooner after grafting
94 than movement from root-to-shoot (Fig. 1l). As rice seedlings aged, the rate of graft formation
95 decreased (Fig. 1m) suggesting that more embryogenic tissues support higher rates of fusion.
96 Taken together, the data from wheat and rice are consistent with fully functional graft unions
97 having formed.
98

Gene expression during grafting

We next sought to investigate changes in gene expression associated with graft formation in monocotyledons. Using rice, we undertook deep-sequencing of RNA at one, three, five, and seven days after grafting from mesocotyl tissue on either side of the graft junction, as well as analogous tissue of non-grafted, or wounded controls (Fig. 2a, Extended Data Fig. 4a, b, Supplementary Table 2). Hundreds of differentially expressed genes (DEGs) were detected between grafted, non-grafted, and wounded samples at each timepoint (Fig. 2b, Extended Data Fig. 4c, Supplementary Table 3). As in dicotyledons[8,9], Gene ontology (GO) terms (Extended Data Fig. 4d, Supplementary Table 4) and specific genes (Fig. 2c, Extended Data Fig. 4e) associated with processes such as non-vascular cell division to fuse the ground/parenchyma tissue, cell-cell adhesion, hormone signaling, and vascular connection establishment were enriched in grafted rice compared with controls. These data therefore indicate common molecular responses unify grafting in monocotyledons and dicotyledons. Not only did the expression of rice genes associated with biological processes previously linked to grafting in *Arabidopsis* change (Fig. 2c) but in some cases rice orthologs of *Arabidopsis* genes known to respond to grafting showed the same response (Fig. 2c, Extended Data Fig. 4e). For example, in *Arabidopsis*, the functionally redundant *NAC* transcription factors (TFs) *ANAC071* and *ANAC096*, the *AP2/ERF* TFs *RAP2.6L* and *WIND1*, and *XYLOGLUCAN ENDOTRANSGLUCOSYLASE/HYDROLASE* genes *XTH19* and *XTH20* are critical for wound healing and act to promote cell division of the ground tissue[10–12]. We found that rice orthologs for these genes were upregulated relative to non-grafted controls during graft formation (Fig. 2c).

Genes involved in cell cycle, division, cell wall remodeling and elongation showed early signs of activation after grafting (Extended Data Fig. 5a, Supplementary Table 5). Genes involved in the cell cycle such as *CYCLINS*, *RETINOBLASTOMA* and *GROWTH*

REGULATING FACTORS, as well as cell expansion genes in the *SMALL AUXIN UP-REGULATED*, *EXPANSIN* and *GLYCOSYLHYDROLASE* families showed higher transcript abundance early in graft formation (Extended Data Fig. 5b, Supplementary Table 6). Consistent with these patterns in transcript abundance, cells of both the scion and rootstock elongated after grafting (Fig. 1k). These data suggest that the gap between rootstock and scion at the graft interface (Fig. 1j) is filled by a combination of cell division and elongation, a phenomenon matching that in dicotyledon grafts and incisions[9,13].

In dicotyledons cambium is thought to be important for graft formation, but monocotyledons including rice lack vascular cambium. We therefore investigated whether pro-cambium or cambium-like activity occurred during rice grafting. Rice orthologs of pro-cambium related TFs *LONESOME HIGHWAY* (*OsbHLH150*) and *MONOPTEROS* (*OsARF5*) were not differentially expressed between grafted and non-grafted rice (Extended Data Fig. 4e). Similarly, rice orthologs of *Arabidopsis* cambium-related genes *WUSHCHEL HOMEOBOX 4*, *PHLOEM INTERCALATED WITH XYLEM* (*OsPXY*) and *SMAX1-LIKE5* (*OsSMXL5*) were not differentially expressed, although a non-significant increase was detected one day after grafting. However, Os*PXY*, *OsSMXL5*, *OsARF5*, and *ABNORMAL VASCULAR BUNDLES* transcripts showed a peak one day after grafting in grafted and non-grafted rice compared with wounded controls suggesting they may serve to prime vascular formation (Extended Data Fig. 4e). In dicotyledons, the cambium differentiates to phloem and xylem and some vascular-related genes were upregulated in rice. For instance, *OsDOF7/11* the rice ortholog of *Arabidopsis* cambium-related *HIGH CAMBIAL ACTIVITY 2* was upregulated during grafting (Fig. 2c, Extended Data Fig. 4e). *OsDOF7/11* is involved in vascular development and induces expression of *SUCROSE TRANSPORTER* and *SWEET* genes in the phloem[14]. *OsNAC85* is similar to *Arabidopsis ANAC075* that regulates xylem tracheary element differentiation[15] and was upregulated during graft healing. Cambium- and vascular-related genes are rapidly induced in

149 *Arabidopsis*[9] and *Nicotiana*[16] grafts and in our rice datasets related transcription factors were
150 induced early during graft formation indicating they might play an important role in vascular
151 specification (Extended Data Fig. 6a, Supplementary Table 7). For example, *WOUND-*
152 *INDUCED POLYPEPTIDE 6* and *OsWIP6-LIKE* were upregulated (Fig. 2b, c) similar to their
153 *Arabidopsis* orthologs (AT3G57670 and AT1G08290)[9]. Collectively, these data suggest broad
154 regulatory conservation between rice and *Arabidopsis* grafting.

155 As well as similarities between the grafting response in rice and *Arabidopsis*, we also
156 detected molecular changes that to our knowledge have not been reported previously. This
157 included down-regulation of certain microRNA precursor genes (pre-miRNAs) during grafting
158 (Extended Data Fig. 6b). miR166 is a negative regulator of vascular development that functions
159 to reduce expression of HOMEOBOX DOMAIN-LEUCINE ZIPPER (HD-ZIP) TFs involved
160 in xylem development[17]. During rice graft formation, *pre-miR166* became less abundant, and
161 the HD-ZIP TFs *HOMEOBOX 6* and *TRANSCRIPTION FACTOR 1* were up-regulated
162 (Extended Data Fig. 6b). Moreover, abundance of pre-microRNA genes *miR159* and
163 *miRNA169* which are stress-induced regulators of growth[18] decreased whilst putative targets
164 such as two R2R3-MYBs, increased during grafting (Extended Data Fig. 6b). Across all
165 timepoints, several *EARLY NODULIN* (*ENOD*) *93* genes were up-regulated after grafting
166 (Extended Data Fig 6c). *ENOD* or *ENOD-like* genes are involved in nodule development in
167 legumes but have largely unknown roles in other lineages. In palm, *ENOD93* is stimulated by
168 auxin and is essential for embryogenic callus formation[19]. Re-analysis of publicly available
169 data indicated that seven of the twenty-two *ENOD* genes in *Arabidopsis* were highly up-
170 regulated during graft formation (Extended Data Fig. 6c). This finding suggests that this gene
171 family plays a yet unidentified role in both monocotyledon and dicotyledon grafting.

172 Genes involved in meristem proliferation and plant growth in monocotyledons were induced
173 during grafting (Fig. 2b). These included the auxin-stimulated *HAIRY MERISTEM 1*

(*OsHAM1*) and *OsHAM2* which function together to promote cell differentiation in meristems[20], *AUXIN-REGULATED GENE INVOLVED IN ORGAN SIZE* which increases growth[21], and the *GIBBERELLIC ACID STIMULATED TRANSCRIPT* gene *OsGASR1*, and *GA INSENSATIVE DWARF 1* genes *OsGID1L2* and *OsGID1L2-like* involved in cell proliferation and elongation[22,23]. In order to validate an association between hormone responsive genes and monocotyledon grafting, we tested the effect of blocking their action as well as application of exogenous phytohormones. Paclobutrazol (PBZ), a gibberellin biosynthesis inhibitor, or the auxin transport inhibitor 2,3,5-triiodobenzoic acid (TIBA) significantly reduced graft union formation, whilst application of gibberellin and auxin enhanced graft formation in rice from 53 % to 78 % seven days after grafting (Fig. 2d). Taken together, these data point to similarities in how gene expression is reprogrammed during grafting in monocotyledons and dicotyledons. Furthermore, despite their phylogenetic distance, some *Arabidopsis* and rice orthologs responded in the same way to grafting.

Widespread grafting in monocotyledons

We next tested whether grafting was possible in other taxonomic groups of monocotyledons. Of the eleven monocotyledonous orders (Fig. 3a), dozens of species across nine phylogenetically diverse orders could self-graft (Fig. 3b, Supplementary Table 1). These spanned all three monocotyledonous clades: the Commelinids, Lilioids and Alismatids (Extended Data Fig. 7) and included important crop species such as pineapple, banana, onion, tequila agave, oil palm and date palm (Fig. 3b, c, Extended Data Fig. 7). Date palm grafts have been growing normally compared with non-grafted controls for over two years (Fig. 3c) demonstrating long-term stability. Grafts also formed in *Acorus* sp., the lineage that is sister to all other monocotyledons (Extended Data Fig. 7). Collectively, these data indicate grafting is

198 conserved across annual and perennial monocotyledons from early- (basal) to late-branching
199 taxa that diverged as much as 130 million years ago[24].

200 Graft compatibility is normally restricted to closely related species with inter-generic grafts
201 such as those observed within the Solanaceae (nightshade) and Cactaceae (cactus) families[16,25]
202 being exceptional. As durum wheat, rice and pearl millet grafted to different genotypes of the
203 same species (Extended Data Fig. 8a, b) we attempted to fuse more distantly related
204 monocotyledons. We found that hexaploid wheat grafted to a range of other species, producing
205 inter-specific unions with durum wheat, inter-generic unions with rye, and inter-tribal unions
206 with oat (Extended Data Fig. 8c, Supplementary Table 1). Additionally, grasses that utilize the
207 C_3 photosynthetic pathway such as wheat, rice and rye grafted to species that use C_4
208 photosynthesis, such as pearl millet and sorghum (Fig. 3d, e, Supplementary Table 1). These
209 species belong to the distantly related PACMAD and BOP clades of the Poaceae (grass family)
210 respectively. Thus, grasses separated by deep-evolutionary time are graft compatible, and
211 compatibility between species that diverged close to the origin of the Poaceae provides
212 evidence that they have may have retained characteristics allowing grafting derived from their
213 common ancestor.

214

215 **Monocotyledon grafting confers benefits**

216 As grafting is commonly used to modify phenotypic properties of the scion we tested
217 whether modifying shoot traits by grafting was possible in monocotyledons. When a wild type
218 rice rootstock was fused to a scion containing a mutation in the *carotenoid cleavage*
219 *dioxygenase 8* gene involved in biosynthesis of strigolactone hormones (Extended Data Fig.
220 9a) this rescued the excessive tillering phenotype caused by strigolactone deficiency[26] (Fig. 4a,
221 b, Extended Data Fig. 9b). These grafts remained intact for the entire lifecycle and self-
222 pollinated seed collected from these grafts reverted to the mutant high tillering phenotype

(Extended Data Fig. 9c, d). These data are consistent with strigolactone traversing the graft union and show that graft transmissible signals can be used to modify shoot traits in monocotyledons.

As grafting can provide resistance to soil-borne pathogens we tested whether this was possible in monocotyledons. Wheat, along with the rest of the Triticeae tribe, lacks resistance to *Gaeumannomyces graminis*, a serious soil-borne fungal pathogen which is responsible for the disease take-all. However, take all does not affect oat due to the biosynthesis of antimicrobial triterpene glycosides known as avenacins that confer broad-spectrum resistance to soil-borne pathogens and fluoresce blue under ultra-violet illumination[27]. Grafting oat rootstocks to wheat scions provided tolerance to this important pathogen (Fig. 4c-f, Extended Data Fig. 10), providing proof-of-principle that grafting monocotyledons can confer agricultural benefits. Such benefits may be important for perennial monocotyledonous crops and include biotic or abiotic stress tolerance provided by resistant rootstocks or by the transmission of resistance from rootstock-to-scion via mobile RNAs, hormones, or proteins.

Discussion

Overall, our findings overturn the consensus that vascular cambium is a prerequisite for graft formation in plants. It appears that the embryonic hypocotyl allows grafting in the majority of monocotyledonous orders. We therefore propose that graft compatibility is unified by the presence of meristematic tissue that can proliferate and merge to form a successful union. Vascular cambium facilitates this process in dicotyledons and gymnosperms, whilst embryonic tissue can achieve the same outcome in monocotyledons perhaps through the presence of tissue that differentiates to vasculature at the graft junction[28]. Embryonic mesocotyl tissue is totipotent and can be used as an explant for monocotyledon regeneration, whose vasculature

247 also forms a cylinder that facilitates alignment. Fusing embryonic tissues of dicotyledons, or
248 gymnosperms may expand their range of graft compatibility.

249 Monocotyledonous species lack secondary growth from cambium tissue, but some species
250 still develop substantial stems by a thickening type of growth. This results from division and
251 enlargement of parenchyma cells of the ground tissue producing new parenchyma from which
252 secondary vascular elements can differentiate[29]. With the proviso that adventitious root
253 formation from stem tissue would have to be controlled[30], the finding that pathogen-resistant
254 rootstocks of oat can be combined with shoots of wheat implies a simple and environmentally-
255 friendly technology for combatting devastating soil-borne diseases, such as Panama disease of
256 banana, or *Ganoderma* basal stem-rot of oil-palm. As grafting is widespread in dicotyledons
257 and gymnosperms, the most parsimonious explanation for our findings is that all seed-bearing
258 plant lineages have the competency to graft.

259

260 **References**

261 1. Mudge, K., Janick, J., Scofield, S. & Goldschmidt, E. E. A history of grafting. *Hortic.*
262 *Rev. (Am. Soc. Hortic. Sci).* **35**, 437–493 (2009).

263 2. Melnyk, C. W. & Meyerowitz, E. M. Plant grafting. *Curr. Biol.* **25**, 183–188 (2015).

264 3. The Plant List. Version 1.1. *Published on the internet* (2013). Available at:
265 http://www.theplantlist.org/. (Accessed: 4th November 2021)

266 4. Calderini, I. M. Essai d'expériences sur la graffe des graminées [Experimental trials on
267 grafting grasses]. *Ann. Sci. Nat. Bot. III* 131–133 (1846).

268 5. Muzik, T. J. & La Rue, C. D. The grafting of large monocotyledonous plants. *Science.*
269 **116**, 589–591 (1952).

270 6. Obolensky, G. Grafting of plant embryos and the use of ultrasonics. *Qual. Plant.*

Mater. Veg. **7**, 273–288 (1960).

7. McCann, M. C. Chimeric plants-the best of both worlds. *Science.* **369**, 618–619 (2020).

8. Melnyk, C. W., Schuster, C., Leyser, O. & Meyerowitz, E. M. A developmental framework for graft formation and vascular reconnection in *Arabidopsis thaliana*. *Curr. Biol.* **25**, 1306–1318 (2015).

9. Melnyk, C. W. *et al.* Transcriptome dynamics at *Arabidopsis* graft junctions reveal an intertissue recognition mechanism that activates vascular regeneration. *Proc. Natl. Acad. Sci. U. S. A.* **115**, E2447–E2456 (2018).

10. Iwase, A. *et al.* The AP2/ERF transcription factor WIND1 controls cell dedifferentiation in *Arabidopsis*. *Curr. Biol.* **21**, 508–514 (2011).

11. Pitaksaringkarn, W. *et al.* XTH20 and XTH19 regulated by ANAC071 under auxin flow are involved in cell proliferation in incised *Arabidopsis* inflorescence stems. *Plant J.* **80**, 604–614 (2014).

12. Asahina, M. *et al.* Spatially selective hormonal control of RAP2.6L and ANAC071 transcription factors involved in tissue reunion in *Arabidopsis*. *Proc. Natl. Acad. Sci. U. S. A.* **108**, 16128–16132 (2011).

13. Matsuoka, K. *et al.* Wound-inducible ANAC071 and ANAC096 transcription factors promote cambial cell formation in incised *Arabidopsis* flowering stems. *Commun. Biol.* **4**, (2021).

14. Wu, Y. *et al.* Rice transcription factor OsDOF11 modulates sugar transport by promoting expression of sucrose transporter and SWEET genes. *Mol. Plant* **11**, 833–845 (2018).

15. Zhong, R., Lee, C., Hahighat, M. & Ye, Z.-H. Xylem vessel-specific SND5 and its homologs regulate secondary wall biosynthesis through activating secondary wall NAC binding elements. *New Phytol.* **4**, 1496–1509 (2021).

16. Notaguchi, M. *et al.* Cell-cell adhesion in plant grafting is facilitated by *β*-1,4-glucanases. *Science.* **369**, 698–702 (2020).

17. Růžička, K., Ursache, R., Hejátko, J. & Helariutta, Y. Xylem development - from the cradle to the grave. *New Phytol.* **207**, 519–535 (2015).

18. Zhao, B. *et al.* Members of miR-169 family are induced by high salinity and transiently inhibit the NF-YA transcription factor. *BMC Mol. Biol.* **10**, (2009).

19. Chan, P. L. *et al.* Early nodulin 93 protein gene: essential for induction of somatic embryogenesis in oil palm. *Plant Cell Rep.* **39**, 1395–1413 (2020).

20. Schulze, S., Schäfer, B. N., Parizotto, E. A., Voinnet, O. & Theres, K. LOST MERISTEMS genes regulate cell differentiation of central zone descendants in *Arabidopsis* shoot meristems. *Plant J.* **64**, 668–678 (2010).

21. Wang, B., Sang, Y., Song, J., Gao, X. Q. & Zhang, X. Expression of a rice OsARGOS gene in *Arabidopsis* promotes cell division and expansion and increases organ size. *J. Genet. Genomics* **36**, 31–40 (2009).

22. Lee, S. C., Kim, S. J., Han, S. K., An, G. & Kim, S. R. A gibberellin-stimulated transcript, OsGASR1, controls seedling growth and *α*-amylase expression in rice. *J. Plant Physiol.* **214**, 116–122 (2017).

23. Ueguchi-Tanaka, M. *et al.* GIBBERELLIN INSENSITIVE DWARF1 encodes a soluble receptor for gibberellin. *Nature* **437**, 693–698 (2005).

24. Eguchi, S. & Tamura, M. N. Evolutionary timescale of monocots determined by the

317 fossilized birth-death model using a large number of fossil records. *Evolution (N. Y).*
318 **70**, 1136–1144 (2016).

319 25. Melnyk, C. W. Plant grafting: Insights into tissue regeneration. *Regeneration* **4**, 3–14
320 (2017).

321 26. Umehara, M. *et al.* Inhibition of shoot branching by new terpenoid plant hormones.
322 *Nature* **455**, 195–200 (2008).

323 27. Mylona, P. *et al.* Sad3 and Sad4 are required for saponin biosynthesis and root
324 development in oat. *Plant Cell* **20**, 201–212 (2008).

325 28. Scarpella, E. & Meijer, A. H. Pattern formation in the vascular system of monocot and
326 dicot plant species. *New Phytologist* **164**, 209-242 (2004).

327 29. Jura-Morawiec, J., Tulik, M. & Iqbal, M. Lateral meristems responsible for secondary
328 growth of the monocotyledons: A survey of the state of the art. *Bot. Rev.* **81**, 150–161
329 (2015).

330 30. Steffens, B. & Rasmussen, A. The physiology of adventitious roots. *Plant Physiol.*
331 **170**, 603–617 (2016).

Figure Legends

Fig. 1. Mesocotyl allows monocotyledon grafting. a, Schematic of grafting. **b**-**e**, Wheat with ß-glucuronidase (GUS) fused to wild type (WT) one week (**b**, **c**) and four months after grafting (**d**, **e**). Bisected plants (**b**, **d**), sections (**c**, **e**). Quantifiation of **b**, and **c** in Extended Data Fig. 2k. **e,** Vasculature between dashed lines. *n*=5. **f**, Scion and rootstock show vascular transport of CFDA across graft junction of wheat seven days after grafting. *n*=10. **g**, **h**, Rice seven days after grafting (**g**), toluidine blue stained section (**h**). *n*=65. **i**, Attachment rate in rice grafts. *n*=82, 59, 77, 65 (1, 3, 5, 7 days after grafting respectively). **j**, Scanning electron microscopy of union formation in rice. *n*=5. **k**, Average length of rice rootstock and scion cells at interface during graft formation. Letters indicate significant groupings (Tukey HSD test, α = 0.05). Longest axis measured on ten cells each side of the junction. *n*=5. **l**, Rice vascular connection determined by transport of CFDA across the junction. *n*=8, 14, 45, 20, 12 (phloem) and *n*=9, 11, 31, 30, 11 (xylem) (4, 5, 6, 7, 10 days after grafting, respectively). **m**, Rice graft attachment rate. *n*=77, 95, 105, 99, 80, 132, 115, 78, 101, 47 (1 through 10 days after grafting). White arrowheads indicate graft junctions (**b-e, g, h, j**). Comparisons were made using mixed effect binomial regression with replicate experiments as a random effect (**i**, **l**, **m**) or two-way ANOVA (**k**). Data are mean ± s.d. of replicate experiments (**i**, **l**, **m**). Violin plots with internal box-and-whisker plots display median, interquartile range (boxes), minima and maxima (whiskers) (**k**). Scale bars represent 1 mm (**b**, **d, g**), or 100 μm (**c**, **e, f**, **h**, **j**).

Fig. 2. Molecular analysis of monocotyledon graft unions. a, Diagram of grafted and non-grafted rice tissue harvested for transcriptome analysis one, three, five, and seven days after grafting. **b**, Normalized expression of grafting-related genes in rice. **c**, Expression of genes associated with graft-related biological processes. Data are mean ± s.e.m, and comparisons made by two-way ANOVA (grafted rice versus non-grafted). *n*=3. **d**, Rates of graft fusion after

treatment with inhibitors of hormone movement, biosynthesis, or exogenous hormone application. Data presented as box-and-whisker plots displaying median, interquartile range (boxes) and minima and maxima (whiskers) of replicate tests, and comparisons made by two-tailed Fisher's exact test. *n*=83 (inhibitor control), 74 (PBZ), 72 (TIBA), 21 (PBZ and TIBA), 67 (hormone control), 67 (GA_3), 80 (2,4-D), 55 (GA_3 and 2,4-D).

Fig. 3. Graft compatibility is widespread in the monocotyledons. **a**, Phylogenetic reconstruction of the eleven orders comprising the monocotyledon clade. Approximate number of species contained in each order are shown in parentheses. Species grafted are shown in bold. The tree was rooted and non-monocotyledon outgroups removed. **b**, Fusion efficiency for grafting diverse crops and ornamentals across the monocotyledon lineage. Grafted plants were evaluated seven to sixty days after grafting by both pulling scion and rootstock and sectioning the graft junction. **c**, Representative images of grafted perennial monocotyledons. Inserts show sections (tequila agave and banana) or enlargement of the graft junction (date palm). *n*=4 (tequila agave), *n*=6 (banana), *n*=6 (date palm). **d**, Rates of fusion among C_3 and C_4 photosynthetic cereal crop species. **e**, Representative images of grafts between C_3 and C_4 cereal species seven days after grafting (quantified in **d**), and longitudinal sections though the graft junctions (inserts). *n* values for grafting rates listed in each panel (**b**, **d**). White arrowheads indicate graft junctions (**c**, **e**). Scale-bars represent 1 cm (**c,** banana, date palm) 1 mm (**c**, tequila agave), 200 μm (**c**, tequila agave, banana inserts), 0.5 mm (**e**).

Fig. 4. Grafting monocotyledons modifies phenotypes. **a**, **b**, Complementation of rice defective in strigolactone hormone biosynthesis. **a**, Phenotype of self-grafted wild type (WT) rice (left), self-grafted *ccd8* strigolactone biosynthesis mutant (center), and intra-specific grafts between a *ccd8/ccd8*-scion and WT-rootstock (right) at maturity. **b**, Quantitation of tillering in

each graft combination of **a**. Letters denote significant ($P < 0.05$) groupings among graft types (pairwise *t*-tests with adjusted *P*-values by the Bonferroni multiple testing correction). Data are presented as mean ± s.d. *n*=8. **c**-**f**, Grafting wheat to oat confers tolerance to take-all disease. **c,** Representative images of self-grafted oat, self-grafted wheat, and inter-tribal grafts between a wheat scion and an oat rootstock (**c**) and root tips (**d**) 21 days after *G. graminis* var. *tritici* infection and 28 days after grafting. *n*=6. **d**, Blue fluorescence derived from avenicins were detectable in oat root tips. *n*=6. Ultra-violet (UV), brightfield (BF), and merged images of root tips. **e**, Percent plants not showing brown necrosis in the scion 21 days after inoculation. *n*=6. **f**, Quantification of blue fluorescence from avencins in root tips taken under identical exposure settings, normalized by integrated pixel density of the UV channel divided by the BF channel displayed as box-and-whisker plots displaying median, interquartile range (boxes) and minima and maxima (whiskers). Letters indicate significant groupings (Tukey test, $\alpha = 0.05$). *n*=6. Comparisons made by two-way repeated measures ANOVA (**b**), two-tailed Fisher's exact test (**d**), or one-way ANOVA (**e**). Scale bars represent 5 cm (**a**), 1 mm (**b**), or 500 μm (**d**).

Materials and Methods

Seed sterilization, germination, and growth conditions

Mature cereal seeds were surface sterilized in 70 % (v/v) ethanol for two minutes, shaken in 1-4 % (v/v) sodium hypochlorite containing 0.01 % (v/v) Tween-20 for 30-40 minutes at ambient room temperature, and then rinsed thoroughly in sterile Milli-Q® water. Seeds were transferred to moist filter paper in darkness and were grafted usually after 12-16 h once partial germination had occurred, alternatively, grafting cereals can be undertaken up to ten days after sterilization/germination. We did not evaluate timepoints after this. Banana and date palm seeds were sterilized by complete submersion in 4 % (v/v) plant preservative mixture™ (PPM, Apollo Scientific) with gibberellic acid (GA_3) for 72 h in a 28 ºC shaking incubator prior to

germination. Banana was placed in a 10 $mg \cdot L^{-1}$ GA_3 solution to initiate germination, whilst a 100 $mg \cdot L^{-1}$ GA_3 solution was used for date palm. Any seeds floating after 72 h were discarded. Following this, seeds that had sunk were placed onto moist filter paper at 30 ºC in darkness until germination occurred, usually two weeks. After grafting, temperate species (*e.g.*, wheat, rye, and oat) were grown at 25.5 / 23.5 ºC (day / night), whilst the tropical species (*e.g.*, rice, pearl millet, sorghum, maize, banana, and date palm) were grown at constant 28 ºC at a light intensity of 60-100 µmol m^{-2} s^{-1} both with a 16 h light photoperiod. When a tropical species was grafted to a temperate species (*e.g.*, wheat grafted to sorghum), the temperate growth condition was used. Other monocotyledonous species were sterilized and germinated according to methods listed in Supplementary Table 8.

All manipulations were performed in a laminar flow cabinet, where seeds were handled only with forceps sterilized in a glass bead sterilizer at 250 ºC or by flaming. In all cases, moisture levels were maintained by addition of autoclaved Milli-Q® water if filter paper within petri plates became visibly dry. Plates were sealed with parafilm (Amcor, UK).

Grafting procedures

Grafting cereals

Grafting of cereals was undertaken by making a transverse cut through the mesocotyl and exchanging embryonic pieces (plumule or radicle) between seeds with a 0.1 mm thick razor blade or a sharp 1-1.5 mm diameter biopsy puncher. Grafted seeds were kept on moist, sterile filter paper. Those exhibiting further growth of both scion and rootstock after five to seven days are good candidates for successful grafts. These were confirmed either by destructive evaluation or by examination of the whole plants under a dissecting microscope (see Video 1). A skilled researcher should be able to perform 80-100 grafts in one hour. See Videos 2 and 3 for demonstrations of this technique for several species.

Grafting diverse monocotyledon species

The biopsy punch method described above and demonstrated in Videos 2 and 3 is effective for Poaceae species because the plumule-radicle axis is enlarged sufficiently for the mesocotyl to be cut before germination occurs. However, in most other monocotyledons, the plumule-radicle axis remains microscopic prior to germination and does not enlarge until it is pushed out of the seed at one end of the elongating cotyledon[31,32]. This renders the biopsy punch method unfeasible for most other monocotyledons outside Poaceae. However, we developed alternative approaches that were able to graft numerous other species of monocotyledon. These are described next.

Non-grass species can instead be grafted by severing and re-joining germinated seedlings at the hypocotyl (the equivalent to the mesocotyl in grasses) once the plumule-radicle axis has elongated. This can be performed days, and indeed weeks for slow growing species, after germination. This method was employed for date palm, and all non-grass species listed in Fig. 3a. Specific germination procedures for these species are listed in Supplementary Table 8.

Specimens for grafting were severed at the hypocotyl using either a fine razor blade with a 0.1 mm blade thickness, or a five mm long, 15º-angled stab knife (Sharpoint™, UK). Razor blades were autoclaved prior to use, while stab knives were sanitized in 70 % (v/v) ethanol and allowed to dry. The severed halves of the seedling were gently pressed together using sterilized fine forceps. In the majority of cases, a very small quantity (< 1 µL) of high viscosity cyanoacrylate superglue ('Stick2 Gel Superglue', Everbuild, UK, or 'High Viscosity Super Glue', Bond-It, UK), first allowed to dry for 10-30 minutes to further increase viscosity, was applied across the outside of graft junction using a sterile pipette tip to hold the seedling halves in contact ahead of fusion occurring. Careful precision in applying the adhesive was taken to

ensure that glue did not seep into the graft junction. Alternatively, silicone tubing of the precise diameter of the hypocotyl can be used to hold the tissue together while fusion takes place.

To permit later manipulation, specimens were grafted on autoclaved nitrocellulose membranes (Biorad, UK) over two layers of Whatman® filter paper (Fisher, UK), to which roots cannot adhere. Plate moisture was kept low during grafting to prevent water wicking into the graft junction, which can inhibit fusion. All grafting steps were conducted in a laminar flow cabinet using a dissecting microscope.

Grafted plants, along with non-grafted seedlings serving as controls, were grown under the same conditions in which they were germinated (Supplementary Table 8), with the exception of plants germinated in the dark. These were grown at the same temperature but were transferred to light with a 16 / 8 h long-day photoperiod. Moisture levels were visually monitored and adjusted as necessary by addition of autoclaved deionized water. Lastly, *Ammomum subulatum* and *Puya raimondii* were transferred to half-strength MS medium (0.8 % w/v agar, pH 5.8) eight days after grafting to provide additional nutrients.

For banana var. Cavendish and var. Pahang grafting, newly formed shoots were micropropagated in tissue culture as described previously[33]. Very young banana shoots produced from a shoot connected to corm tissue from which it differentiated were removed placed in direct contact with severed embryonic roots derived from from wild banana seed or tissue culture corm tissue, and held together with a sterile grafting clip or silicone tube of the same diameter as corm, and placed on minimal media (2.205 $g \cdot L^{-1}$ Murashige and Skoog (MS) salts, 6 $g \cdot L^{-1}$ agar, pH 5.8) to fuse.

Graft evaluation

Fusion rate assessment

To assess the attachment rate of grafts, destructive methods were used. First, plants were pulled gently with two sets of forceps gripping the scion and rootstock and pulling in opposition. Anything that separated easily was considered not grafted. Grafted plants that did not separate were subsequently hand sectioned by trimming the plant approximately 0.25 cm above and below the graft junction and then a longitudinal slice perpendicular to the junction through the grafted plant was made. The tissue was then inspected under a dissection microscope for evidence of fusion. Any tissue clearly fused was considered grafted. See Video 1 for a demonstration of this process. The rate of grafting was determined as the number of plants fused (not separated when pulled and then hand sectioned) divided by the total number of embryos or plantlets grafted. As grafting can be performed on pre- or partially germinated seeds, we evaluated the germination rate as well. For hormone inhibitor and exogenous hormone treatment assays on graft union formation in rice (see Fig. 2e), the rates of grafting were determined as the number of fused plants divided by the total number of germinated plants. This was because certain hormones (*i.e.*, gibberellin) or inhibitors (*i.e.*, PBZ) affect the germination rate. A full description of grafting rates can be found in Supplementary Table 1.

GUS and toluidine blue staining

To visualize activity of the GUS reporter, plants were placed in a 5-Bromo-4-chloro-3-indolyl-β-D-glucuronide (X-gluc) GUS staining solution (0.1 M NaH_2PO_4 / Na_2HPO_4 buffer (pH 7.0), 0.5 mM potassium ferrocyanide, 0.5 mM potassium ferricyanide, 0.06 % (v/v) Triton X-100, 10 mM Na_2 EDTA (pH 8.0), 0.5 $g \cdot L^{-1}$ X-gluc) and incubated overnight at 37 ºC, prior to being cleared in 70 % (v/v) ethanol. To visualize sections of graft junctions, tissue was first sectioned, cleared overnight in 70% (v/v) ethanol, rinsed three times with water, stained in a 0.1 % (w/v) toluidine blue solution for 5-10 minutes followed by three rinses with water.

505 *Vascular connectivity assays*

506 To assess functional vascular connections across graft sites, 5(6)-carboxyfluorescein
507 diacetate (CFDA) was used as described previously[34], between four to fourteen days following
508 grafting. For xylem assays, the roots of grafted plants were cut off two cm below the junction
509 and inserted into a solidified line of CFDA-agar (2.205 $g \cdot L^{-1}$ MS salts, 8 $g \cdot L^{-1}$ Bactoagar, and
510 1 mM CFDA, pH 6.7). For phloem assays, the shoot was cut 2 cm above the junction and 2 µL
511 of molten CFDA-agar was applied to the wounded site. Care was taken not to touch any other
512 part of the plant with CFDA-agar. After one to two hours, plants were viewed under a Leica
513 M205 FCA fluorescence stereo microscope fitted with a GREEN FLUORESCENT PROTEIN
514 (GFP) filter (Leica Microsystems, Newcastle, UK), and imaged as a Z-stack with LAS X
515 software (Leica Application Suite, Newcastle, UK). To view the entire seedling, some images
516 were stitched together in Fiji (ImageJ version 2.0.0) (see Extended Data Fig. 3e-l). As the stem
517 tissue of certain monocotyledons (*e.g.*, wheat) are thick, a longitudinal slice perpendicular to
518 the junction through the grafted plant from the non-CFDA inoculated half of the graft towards
519 the CFDA applied half was made in order to better visualize the internal vasculature (see
520 Extended Data Fig. 2l-s). Confocal images were obtained on a Zeiss LSM780 microscope and
521 images processed using Fiji software. Non-grafted plants treated with CFDA-free agar (mock
522 solution) acted as negative controls, allowing any autofluorescence in the CFDA (GFP)
523 channel to be detected.

524

525 *Electron microscopy*

526 For electron microscopy around two mm^2 of *O. sativa* graft junctions were excised with a
527 razor blade and fixed immediately in 2 % (v/v) glutaraldehyde and 2 % (w/v) formaldehyde in
528 0.05-0.1 M sodium cacodylate (NaCac) buffer (pH 7.4) containing 2 mM calcium chloride.
529 Samples were vacuum infiltrated overnight, washed five times in deionized water, and post-

fixed in 1 % (v/v) aqueous osmium tetroxide, 1.5 % (w/v) potassium ferricyanide in 0.05M NaCac buffer for three days at 4 °C. After osmication, samples were washed five times in deionized water and post-fixed in 0.1 % (w/v) thiocarbohydrazide in 0.05M NaCac buffer for twenty minutes at room temperature in the dark. Samples were then washed five times in deionized water and osmicated for a second time for one hour in 2 % (v/v) aqueous osmium tetroxide in 0.05 M NaCac buffer at room temperature. Samples were washed five times in deionized water and subsequently stained in 2 % (w/v) uranyl acetate in 0.05 M maleate buffer (pH 5.5) for three days at 4 °C and washed five times afterwards in deionized water. Next, samples were dehydrated in an ethanol series, transferred to acetone, and then to acetonitrile. Samples were then embedded in Quetol 651 resin mix (TAAB Laboratories Equipment Ltd). For scanning electron microscopy (SEM), ultrathin-sections were placed on plastic coverslips which were mounted on aluminum SEM stubs, sputter-coated with a thin layer of iridium and imaged in a FEI Verios 460 scanning electron microscope. For light microscopy, thin sections were stained with methylene blue and imaged by an Olympus BX41 light microscope with a mounted Micropublisher 3.3 RTV camera (Q Imaging).

Exogenous hormone and inhibitor assays

To assess the effect of auxin and gibberellin hormones involved in monocotyledon graft formation (*e.g.*, Fig. 2e), plants were grafted and placed onto minimal media (half strength MS salts, 6.5 $g \cdot L^{-1}$ agar, pH 5.8, autoclaved at 121 ºC for a total sterilization time of 12 minutes) with either 5 µM gibberellic acid (GA_3), 5 µM of the auxin 2,4-Dichlorophenoxyacetic acid (2,4-D), or a combination of both hormones. GA_3 was dissolved in water and added to the media as a filter-sterilized solution after autoclaving, whereas 2,4-D was pre-dissolved in 1 N NaOH and co-autoclaved with the media. To assess the effect of auxin and gibberellin hormone inhibitors involved in monocotyledon graft formation, plants were grafted and placed onto

buffered minimal media (half strength MS salts, 0.5 $g \cdot L^{-1}$ 2-(N-morpholino) ethanesulfonic acid (MES), 6.5 $g \cdot L^{-1}$ agar, pH 5.8, autoclaved at 121 ºC for a total sterilization time of twelve minutes) with either 100 µM of the gibberellin biosynthesis inhibitor, Paclobutrazol (PBZ), 100 µM of the auxin transport inhibitor, 2,3,5-triiodobenzoic acid (TIBA), or a combination of both inhibitors. PBZ powder was added into the buffered minimal media and co-autoclaved, whereas TIBA was pre-dissolved in 1 N NaOH and added as a filter-sterilized solution after autoclaving. In both cases, grafts on either minimal media or buffered minimal media containing no hormones or inhibitors were used as controls, respectively.

Grafting reproducibility

Grafts within the monocotyledons presented herein were performed over a seven-year timeframe (2014-2021) at three different institutes (University of Cambridge, NIAB, and Swedish University of Agricultural Sciences) by six different researchers (G.R., A.T., P.S., M.R.W.J., A.K.N., and C.M.). In all years, all locations, and by all researchers, grafts were successful, demonstrating that these techniques are transferable and reproducible.

Gene expression analysis

RNA library prep and sequencing

Total RNA from 0.5 mm on either side of the graft junction or analogous regions of wounded, or non-grafted rice was extracted using Arcturus Picopure RNA extraction kit (ThermoFisher Scientific, UK) with on-column DNaseI treatment according to the manufacturer's protocol. RNA integrity and quality of samples were assessed using 2100-Bioanalyzer (Agilent Technologies, USA) with an Agilent Bioanalyser RNA Pico assay and QuBit (ThermoFisher Scientific, UK), respectively. Only samples with RNA Integrity Number (RIN) ≥5 were selected to be sent for library preparation and further 150 bp paired end Illumina

sequencing by Novagene, UK. A total amount of 1 μg RNA per sample was used as input material for the RNA sample preparations. Sequencing libraries were generated using NEBNext® UltraTM RNA Library Prep Kit for Illumina® (NEB, USA) following manufacturer's recommendations and index codes were added to attribute sequences to each sample. Briefly, mRNA was purified from total RNA using poly-T oligo-attached magnetic beads. Fragmentation was carried out using divalent cations under elevated temperature in NEBNext First Strand Synthesis Reaction Buffer (5X). First strand cDNA was synthesized using random hexamer primer and M-MuLV Reverse Transcriptase (RNase H-). Second strand cDNA synthesis was subsequently performed using DNA Polymerase I and RNase H. Remaining overhangs were converted into blunt ends via exonuclease/polymerase activities. After adenylation of 3′ends of DNA fragments, NEBNext Adaptor with hairpin loop structure were ligated to prepare for hybridization. In order to select cDNA fragments of preferentially 150-200 bp in length, the library fragments were purified with AMPure XP system (Beckman Coulter, Beverly, USA). Then 3 μl USER Enzyme (NEB, USA) was used with size-selected, adaptor- ligated cDNA at 37 °C for fifteen minutes followed by five minutes at 95 °C before PCR. PCR was performed with Phusion High-Fidelity DNA polymerase, Universal PCR primers and Index (X) Primer. Lastly, PCR products were purified (AMPure XP system) and library quality was assessed on the Agilent Bioanalyzer 2100 system.

Clustering

The clustering of the index-coded samples was performed on a cBot Cluster Generation System using PE Cluster Kit cBot-HS (Illumina, UK) according to the manufacturer's instructions. After cluster generation, the library preparations were paired-end sequenced on an Illumina NexSeq 500 machine.

Quality control

Raw data (raw reads) of FASTQ format were first processed through fastp. In this step, clean data (clean reads) were obtained by removing reads containing adapter and poly-N sequences and reads with low quality from raw data. At the same time, Q20, Q30 and GC content of the clean data were calculated. All the downstream analyses were based on clean data with high quality.

Mapping to reference genome and quantification

Rice reference genome (Os-Nipponbare-Reference-IRGSP-1.0) and gene model annotation (RAP-BD) files were downloaded from genome website browser (NCBI/UCSC/Ensembl) directly. Paired-end clean reads were mapped to the reference genome using HISAT2 software. HISAT2 uses a large set of small GFM indexes that collectively cover the whole genome. These small indexes (called local indexes), combined with several alignment strategies, enable rapid and accurate alignment of sequencing reads.

Featurecounts was used to count the read numbers mapped of each gene, including known and novel genes. And then RPKM of each gene was calculated based on the length of the gene and reads count mapped to this gene. RPKM, Reads Per Kilobase of exon model per Million mapped reads, considers the effect of sequencing depth and gene length for the reads count at the same time.

Differential expression analysis

Differential expression analysis between two conditions/groups (three biological replicates per condition) was performed using DESeq2 R package. DESeq2 provides statistical routines for determining differential expression in digital gene expression data using a model based on the negative binomial distribution. The resulting *P* values were adjusted using the Benjamini

and Hochberg's approach for controlling the False Discovery Rate (FDR). Genes with an adjusted *P* value < 0.05 found by DESeq2 were assigned as differentially expressed.

GO enrichment analysis

Gene Ontology (GO) enrichment analysis of differentially expressed genes was implemented by the 'clusterProfiler' R package, in which gene length bias was corrected. GO terms with corrected *P* value < 0.05 were considered significantly enriched by differential expressed genes.

Take-all disease screening

Gaeumannomyces graminis var. *tritici* was grown on half-strength potato dextrose agar (PDA) at 20 ºC under a 12 h dark 12 h near-UV light cycle as previously described[35,36]. Seven days after grafting, wheat and oat grafts were transferred into individual sterile cylindrical containers with sealed lid containing 60 mL of inoculation media (2.205 g·L-1 MS salts, 3.5 g·L-1 phytagel, pH 5.8) and organized in a completely randomized design within a positive pressure spore-proof growth room at 20 ºC with a 16 h photoperiod. A thin layer of partially dry high viscosity cyanoacrylate glue (Bond It, UK) was applied with a fine brush to graft junctions seven days after grafting to reduce production of adventitious roots induced by the relatively high humidity in the containers. The glue did not cause any microbial contamination on the media. A one cm diameter PDA plug of *G. graminis* var. *tritici* was placed directly on top of the root of the grafted seedlings to ensure the pathogen was in contact with the plant. Resistant or susceptible phenotypes were evaluated three weeks after inoculation. At this stage, susceptible wheat controls showed visible disease progression: roots and stem were black and necrotic consistent with previously described disease symptoms[37]. Plants with obvious necrosis on roots which crossed the graft junction were qualitatively counted as susceptible.

655

656 **Statistical analysis**

657 For all statistical tests, individual plants were considered experimental units in a completely
658 randomized design or a completely randomized block design. Data were analyzed in R (version
659 3.6.1). The R packages 'tidyverse', 'ggplot2', 'mgcv', 'dplyr', 'ggpubr', 'car',
660 'multcompView', 'rstatix', 'lsmeans', and 'lme4' were used for data analysis and downloaded
661 via the Install Packages Tool in RStudio (version 1.2.1335). Two-tailed Fisher's exact test (α
662 = 0.05) was used to evaluate differences in grafting frequency among intra-specific wheat
663 grafts, exogenous hormone or inhibitor treated rice grafts, or wheat-oat inter-tribal grafts (*e.g.*,
664 Fig. 2e, Fig. 4e, Extended Data Fig. 1k).

665 One-way analysis of varianace (ANOVA) was used to evaluate the normalized blue
666 fluorescence in root tips of wheat and oat grafts challenged with the pathogen *G. graminis* var.
667 *tritici*, whereby the Tukey Post Hoc Test (α = 0.05) was used for mean separation (*e.g.*, Fig.
668 4f). Two-way ANOVA was used to evaluate cell elongation differences between scion and
669 rootstock graft interface cells and gene expression differences between grafted and non-grafted
670 or grafted and wounded rice plants (e.g., Fig. 1k, Fig. 2c, Extended Data Figs. 4e, 6b, c). Two-
671 way repeated measures ANOVA was used to evaluate strigolactone mutant and wild type grafts
672 (*e.g.*, Fig. 4b and Extended Data Fig. 9b) whereby pairwise *t*-tests with adjusted *P*-values by
673 the Bonferroni multiple testing correction method (α = 0.05) were used for mean separation.
674 Null hypotheses were rejected for specific ANOVAs with $P \leq 0.05$. Levene's test was used to
675 evaluate equal variance and was centered at the mean using the 'car' package in R. All two-
676 way repeated meaures ANOVA analyses showed equal variance ($P > 0.05$), except for the
677 number of tillers at eight and fourteen days after grafting in Fig. 4b, and thus these data at these
678 time points were not analyzed. The Shapiro-Wilk Test was used to evaluate normal distribution

of the raw data and ANOVA residuals for which all populations showed normally distributed data ($P > 0.05$). All observations came from independent random sampling.

A mixed effect binomial model was fitted to attachment rates in grafted rice data to test the hypothesis that the proportion of successful attachments varied with the length of time since the germination took place or time since grafting had taken place (variable: Days), whilst taking into account the blocking effect of different replicate experiments as a random effect (*e.g.*, Fig. 1i, l, m, Extended Data Fig. 3s, t). The analysis was carried out using the 'lme4' package in R. A likelihood ratio test was used to determine statistically significant effects. We included source data and R scripts for these analyses in GitHub: https://github.com/GregReeves/Reeves2021_MonocotGrafting.

Phylogenetic reconstructions

In order to gather data, two datasets were constructed: one consisting of taxa sampled across the monocotyledons, and the other of taxa sampled across the family Poaceae. For both datasets five loci (*rbcL*, *matK*, *ndhF*, *rpoC2* and the internal transcribed spacer region (ITS)) were collected from genbank. Sampling was conducted in a manner that broadly and evenly samples major clades. For the monocotyledon dataset, this resulted in 109 monocot ingroup taxa, and sixteen outgroup taxa spanning flowering plants. For the Poaceae dataset, this resulted in 90 Poaceae taxa with five outgroups chosen from other families within the order Poales. Alignment for both the monocotyledon and the Poaceae datasets, the loci *rbcL*, *matK*, *ndhF* and *rpoC2* were aligned using PRANKv.170427[38] with default settings. This same method was used to align the ITS locus for the Poaceae dataset. For the ITS locus of the full monocotyledon dataset, the sequences were first divided into their respective families and aligned using PRANK with default settings, then these alignments were merged using the (--merge) option

of the program MAFFT v7.471[39]. This was done to accommodate the rapid rate of molecular evolution associated with ITS at such a deep time scale.

In order to infer trees for each respective dataset, the sequences were concatenated into a supermatrix using pxcat from the program Phyx[40]. The maximum likelihood tree was inferred using RAxML-NG v0.9.0[41] with the supermatrix partitioned by loci and the GTR model of evolution with gamma rate variation applied to each locus. The tree was rooted using figtree (v1.4.4) and the outgroups removed.

In order to date each tree, the rooted tree consisting of only the ingroups was dated using penalized likelihood as implemented in TreePL v1.0[42]. The minimum and maximum dates were based on the confidence intervals of the possible dates available from TimeTree[43]. In the case of the full monocotyledon dataset, this was done using 32 calibrations, and in the case of the Poaceae dataset, eleven calibrations were used.

Source data and Phython scripts for these phylogenetic trees have been deposited into a GitHub repository: https://github.com/GregReeves/Reeves2021_MonocotGrafting.

Image preparation

Shoot and root sections of grafted and non-grafted control plants treated with CFDA, and mock solutions were imaged by confocal and fluorescence microscopy (see Fig. 1f, Extedned Data Fig. 2t-y, 3m-r). Raw image files were converted from 8-bit to RBG format with the *Image* > *Type* tool in Fiji (ImageJ version 2.0.0) and were colored with the *Image* > *Lookup Tables* feature corresponding to the green (CFDA) and red (propidium iodide) channels. Finally, these were merged together to form overlays with the *Image* > *Color* > *Merge Channels* tool.

References for materials and methods

31. Tillich, H. J. Ancestral and derived character states in seedlings of monocotyledons. in *Monocots: Systematics and Evolution* 761 (CSIRO Publishing, 2000).

32. Burger, W. C. The question of cotyledon homology in angiosperms. *Bot. Rev.* **64**, 356–371 (1998).

33. Strosse, H., Houwe, I., Panis, B., Jain, S. M. & Swennen, R. Banana cell and tissue culture review. in *Banana Improvement: Cellular, Molecular Biology, and induced Mutations* 1–12 (2004).

34. Melnyk, C. W. Monitoring Vascular regeneration and xylem connectivity in *Arabidopsis thaliana*. in *Xylem: Methods and Protocols* 91–102 (Humana Press, New York, NY, 2017).

35. Hollins, T. W., Scott, P. R. & Gregory, R. S. The relative resistance of wheat, rye and triticale to take-all caused by *Gaeumannomyces graminis*. *Plant Pathol.* **35**, 93–100 (1986).

36. Osbourn, A. E., Clarke, B. R., Lunness, P., Scott, P. R. & Daniels, M. J. An oat species lacking avenacin is susceptible to infection by *Gaeumannomyces graminis* var. *tritici*. *Physiol. Mol. Plant Pathol.* **45**, 457–467 (1994).

37. Chng, S. ., Cromey, M. G. & Butler, R. C. Evaluation of the susceptibility of various grass species to *Gaeumannomyces graminis* var. *tritici*. *New Zeal. Plant Prot.* **58**, 261–267 (2005).

38. Löytynoja, A. & Goldman, N. Phylogeny-aware gap placement prevents errors in sequence alignment and evolutionary analysis. *Science.* **320**, 1632–1635 (2008).

39. Katoh, K. & Standley, D. M. MAFFT multiple sequence alignment software version 7: Improvements in performance and usability. *Mol. Biol. Evol.* **30**, 772–780 (2013).

40. Brown, J. W., Walker, J. F. & Smith, S. A. Phyx: Phylogenetic tools for unix. *Bioinformatics* **33**, 1886–1888 (2017).

41. Kozlov, A. M., Darriba, D., Flouri, T., Morel, B. & Stamatakis, A. RAxML-NG: A fast, scalable and user-friendly tool for maximum likelihood phylogenetic inference. *Bioinformatics* **35**, 4453–4455 (2019).

42. Smith, S. A. & O'Meara, B. C. TreePL: Divergence time estimation using penalized likelihood for large phylogenies. *Bioinformatics* **28**, 2689–2690 (2012).

43. Hedges, S. B., Dudley, J. & Kumar, S. TimeTree: A public knowledge-base of divergence times among organisms. *Bioinformatics* **22**, 2971–2972 (2006).

44. Iwata, N. & Omura, T. Linkage analysis by reciprocal translocation method in rice plants (*Oryza sativa* L.) I. Linkage groups corresponding to the chromosome 1, 2, 3 and 4. *Japanese J. Breed.* **21**, 19-28 (1971).

Acknowledgements

We thank Andy Greenland and Emma Wallington for hosting G.R. at the National Institute of Agricultural Botany, Filomena Gallo and Karin Müller for generating electron microscopy images, Uta Paszkowski for providing *ccd8* mutant rice; Sarah Holdgate for providing a culture of *G. graminis* var. *tritici*; Matt Castle for statistical advice; Mark Tester for supplying tetraploid wheat; Ruth Bates, Ruth Donald, and Kumari Billakurthi for assistance; Mathieu J. Grangé-Guermente, Olga Murshudova, and Natasha Elina for translating foreign language references into English; and lastly to David C. Baulcombe and Alexander M. Jones for providing feedback on this manuscript.

Funding

G.R. was supported by a Gates Cambridge Trust PhD Student Fellowship; G.R. and P.S. by ERC Grant 694733 Revolution and BB/P003117/1 awarded to J.M.H. G.R., A.T. and M.R.W.J. and were supported by a Ceres Agri-Tech Fund award. A.K.N and C.W.M were supported by a Wallenberg Academy Fellowship (KAW 2016.0274) C.M. and C.W.M. were supported by a European Research Council Starting Grant (GRASP-805094).

Author's contributions

G.R. and J.M.H. conceptualized the study. G.R. A.T., P.S., M.R.W.J., A.K.N., C.M. performed grafting experiments. A.T. and P.S. prepared sequencing samples and uploaded data to NCBI. G.R., A.T., M.R.W.J., A.K.N., and C.M. performed vascular connectivity assays. G.R. analyzed data. M.C. and S.B. generated the transgenic GUS-reporter wheat line. M.C., S.B, A.R.B., P.S., C.W.M., and J.M.H. provided advice on experiments. J.F.W. generated phylogenic trees. The study was supervised by A.R.B., C.W.M., and J.M.H. The manuscript was written by G.R. and J.M.H. with contributions from the other authors. All authors discussed the results, reviewed, and approved the final manuscript.

Competing interests

Cambridge Enterprise Ltd. has filed a patent, International Application No. PCT/GB2019/053232, Publication No. WO/2020/099879, titled "Perennial monocotyledon grafting", which includes methods for grafting monocotyledons described in this manuscript published on 22 May 2020, and of which G.R. and J.M.H. are co-inventors. The other authors declare no competing interests.

Data and materials availability

All data are available in the manuscript, extended data and supplementary materials. Deep sequencing reads for grafted, non-grafted, and wounded rice are deposited into the Sequence Read Archive (SRA) of NCBI Accession No.: PRJNA734117. Source data and custom coding scripts for plotting are deposited into the GitHub repository https://github.com/GregReeves/Reeves2021_MonocotGrafting.

Code availability

Source data and custom R scripts used for individual plots and for browsing transcriptome results, as well as source data and Python scripts used for constructing monocotyledon phylogenies are deposited at https://github.com/GregReeves/Reeves2021_MonocotGrafting. None of the custom code are central to conclusions of the manuscript.

Extended Data Figure Legends

Extended Data Fig. 1. Serendipitous discovery of a method that allows grafting of monocotyledons. Immature embryos of wheat (*T. aestivum* - orange) and pearl millet (*P. glaucum* - blue) were grown in tissue culture in order to regenerate a fused plant which may simulate grafting. **a**-**d**, Grafted plants were not generated after simulating grafting by placing halved calli in contact (**a**), pressing two scutella together in media (**b**), slicing scutellar tissue and placing into close contact (**c**), or placing callus into a toroidal arrangement (**d**). However, after removal and exchange of the central part of immature wheat and pearl millet embryos, some germinated into what appeared to be vestigial grafted plants (**e**). Photographs of tissue (left) are next to graphical representations (right). White arrowheads indicate areas of fusion. Scale-bar represents 0.5 cm and applies to all photographs.

Extended Data Fig. 2. Intra-specific wheat grafts form between different genoypes. a, Non-grafted wheat seven days after germination. **b**, Section though the root-shoot interface with the vasculature surrounded by green cells. **c**, Self-grafted wheat seven days after plumule transplantation. **d**, Section though graft junction, with the union interrupting the file of green cells linking shoot and root. Parenchyma and scutellar tissues all were connected. **e**-**h**, Seven day old β-glucuronidase (GUS) wheat (var. Fielder) grafted to wild type (WT) (var. Paragon): grafted seedling (**e**), section through the intra-specific graft junction (**f**), seedling stained with x-gluc (**g**), and ultra-thin section through the stained graft junction (**h**). For **c**-**h**, *n* is quantified in **k**. **i**, The graft site of a GUS-WT wheat grafted plant four months after grafting and after setting seed. **j**, X-gluc stained section through the junction shows continuous vascular strands connecting scion and rootstock between dashed lines. For **i**, **j**, *n*=5. **k**, Rates of fusion between intra-specific GUS-WT grafts one week after grafting, determined destructively by pulling and sectioning (see Video 1 for demonstration). Data are presented as box-and-whisker plots displaying median, interquartile range (boxes) and minima and maxima (whiskers) of pooled data from eleven replicate experiments. Comparisons made by two-tailed Fisher's exact test. **l**-**s**, Vascular connectivity in intra-specific wheat grafts. **l**, **p**, **n**, **r**, The shoot or roots of non-grafted wheat seedlings were inoculated with CFDA-containing agar (**l**, **p**) or a mock agar (**n** and **r**) solutions seven days after germination as controls to observe vascular transport of fluorescence shoot-to-root (**l**) or root-to-shoot (**p**) 1 h following application. **m**, **q**, **o**, **s**, Even after just 1 h following application, CFDA solutions applied to the shoot or roots of intra-specific GUS-WT wheat grafts identified unsuccessful (**o**, **s**) or successful shoot-to-root (**m**) and root-to-shoot (**q**) vascular connectivity as shown by empty green arrowheads. GUS-WT grafts successfully transporting CFDA across the graft junction were stained with X-gluc and are shown to the right of the CFDA channel (**m**, **q**). **t**-**v**, Root cross-sections of the CFDA phloem connection assay seven days after grafting on intra-specific GUS-WT wheat grafts

from **l**, **m**, and **n**, respectively. **w**-**y**, Shoot cross-sections of the CFDA phloem connection assay seven days after grafting. Propidium iodide (PI) was applied on the cross-sections (**t**-**y**), and images were acquired by fluorescence microscopy (**l**-**y**). Negative controls (**n**, **r**, **t**, **w**) showed very little autofluorescence. For **l**-**y**, *n*=10 plants evaluated for CFDA movement in grafts and non-graft controls. White arrowheads indicate the graft junction (**c**-**j**, **m**, **q**, **o**, **s**). BF, bright field channel. Scale bars represent 1 mm (**a**, **c**, **e**, **g**, **i**), 500 μm (**l**-**s**), or 100 μm (**b**, **d**, **f**, **h**, **j**, **t**-**y**).

Extended Data Fig. 3. Grafted rice form functional vascular connections. **a**-**d**, Brightfield (BF) images of toluidine blue (TB) or sodium hydroxide (OH^-) cleared mesocotyl tissue in non-grafted (**a**, **b**) or grafted (**c**, **d**) rice seven days after grafting. The vascular cylinder is shown between dashed lines. For **a**, **b**, *n*=20, and for **c**, **d**, *n*=65. **e**-**l**, Representative BF and confocal microscopy fluorescence images for exogenous CFDA dye application indicate movement across graft junctions from shoot-to-root and root-to-shoot in the vasculature. Non-grafted plants transport CFDA from shoot-to-root (**e**) and from root-to-shoot (**i**). Mock solutions generated no CFDA fluorescence signal (**g**, **k**). Grafted plants transport CFDA from shoot-to-root (**f**) and from root-to-shoot (**j**). Lack of CFDA transport is indicative of failed or delayed graft formation (**h**, **l**). **m**-**r**, Cross-sections indicating CFDA transport to the rootstock (plants from **e**, **f**, and **h**) or scion (plants from **i**, **j**, and **l**) after application of CFDA to the scion or rootstock, respectively, seven days after grafting (grafted five days after germination). All sections were stained with propidium iodide (PI) to visualize shoot or root structure. Images from the CFDA, PI and merged channels are presented. No CFDA fluorescence was detectable in shoots after application of mock agar (**m**). However, when CFDA was provided to roots of non-grafted (**n**) and grafted plants (**o**), signal was detected surrounding xylem tissues of the shoot. Merged images show that CFDA is localized to vascular strands. Enlarged panels show

xylem vessels. No CFDA fluorescence was detectable in roots after application of mock agar (**p**), however, when CFDA was provided to shoots of non-grafted (**q**) and grafted plants (**r**), signal was detected in vascular tissue of the root. Merged images show that CFDA is localized to vascular strands. All images acquired by confocal microscopy. **s**, Attachment rate of rice grafts over time (plants from **e**-**r**). *n*=14, 15, 10, 20, 20, 40, 20, 14, 20 (non-grafted control), *n*=30, 30, 60, 50, 59, 240, 120, 40, 80 (grafted) (1, 2, 3, 4, 5, 6, 7, 10, 14 days after grafting, respectively). **t**, CFDA transport rates in attached grafts from **s** show vascular connectivity increases over the course of seven days. Data are presented as mean grafting rate ± s.d. of three to six replicate experiments (blocking/random effect). *n*=29, 30, 38, 18, 14. (phloem, non-grafted control) *n*=26, 28, 29, 18, 13 (xylem, non-grafted control), *n*=8, 14, 45, 20, 12 (phloem, grafted), *n*=9, 11, 31, 30, 11 (xylem, grafted) (4,5,6,7,10 days after grafting, respectively). Comparisons were made using mixed effect binomial regression with replicate experiments as a random effect (**s**, **t**). White arrowheads indicate graft junctions (**c**, **d**, **f**, **h**, **j**, and **l**). Scale bars represent 1 mm (**e**-**l**), 100 μm (**a**-**d**), or 50 μm (**m**-**r**).

Extended Data Fig. 4. Overview of changes in transcript abundance during the development of graft unions in rice. a, Diagram of non-grafted, wounded, and grafted rice (var. Kitaake) tissue harvested for transcriptome analysis one, three, five, and seven days after grafting. **b**, Three dimensional priniciple component analysis (PCA) of individual biological replicates for non-grafted, wounded, and grafted rice. *n*=3. **c**, Upset plot for differentially expressed genes (DEGs) for grafted versus non-grafted, and grafted versus wounded rice. **d**, The fifteen most up-regulated gene ontology (GO) terms in grafted compared with wounded rice. See Supplementary Table 4 for complete GO term information. **e**, Transcriptional dynamics of genes associated with graft formation. Data are presented as mean ± s.e.m, and as wounded gene expression overlaps significantly with grafted gene expression during

dicotyledon grafting[9], comparisons were made between grafted rice versus non-grafted rice expression by two-way ANOVA. *n*=3. Apart from cambium-maker genes, there was significant overlap of gene expression in rice compared to those associated with dicotyledon grafting.

Extended Data Fig. 5. Dynamics of transcripts from cell expansion and cell division genes during graft formation in rice. a, The fifteen most up-regulated gene ontology (GO) terms relative to each adjacent timepoint. Full list of GO details in Supplementary Table 5. **b**, Z-scores for differentially expressed transcripts of cell expansion genes in the small auxin up regulated (SAUR), EXPANSIN and GLYCOSYLHYDROSE families (left), as well as for cell cycle genes (right) in grafted rice over time. Gene details in Supplementary Table 6.

Extended Data Fig. 6. Specific gene family analysis for rice graft transcriptomics. a, Z-score normalized transcription factors with differential transcript abundance within the *APETALA2/ETHYLENE-RESPONSIVE FACTOR* (*AP2/ERF*); *NO APICAL MERISTEM*, *ARABIDOPSIS TRANSCRIPTION ACTIVATION FACTOR*, *CUP SHAPED COTYLEDON* (*NAC*); *MYELOBLASTOSIS* (*MYB*); *DNA-BINDING ONE FINGER* (*DOF*); and *AUXIN RESPONSE FACTOR* (*ARF*) families between non-grafted and grafted rice over time as determined by significant Two-way ANOVA grouping variable (graft type, $P < 0.05$). Gene details in Supplementary Table 7. **b**, Pre-microRNA transcripts showing reduced expression during grafting and their potential targets involved in plant development. **c**, Early nodulin genes expression during grafting in rice (above) and *Arabidopsis* during grafting. *Arabidopsis* data was adapted from Melnyk et al. 2018[9]. Data are presented as mean ± s.e.m, and comparisons made by two-way ANOVA (grafted rice versus non-grafted expression) (**b**, **c**). *n*=3.

Extended Data Fig. 7. Grafting across all three monocotyledonous groups. a, **b**, Representative images of non-grafted seedlings (**a**), and hand cross sections of plant tissue (**b**) stained with toluidine blue representing species from Alismatid, Lilioid, and Commelinid monocotyledons. **c**, **d**, Representative images of grafted seedlings seven to sixty days after grafting (**c**), and hand cross sections through the graft junction stained with toluidine blue (**d**). Panels in the upper right corner show higher magnification of the graft site (**c**). Non-grafted controls are the same age as grafted plants. For **a**, **b**, *n*=5 and for **c**, **d**, *n*=2 (*Ananas comosus*), *n*=8 (*Costus laevis*), *n*=18 (*Commelina comminis*), *n*=8 (*Beaucarnea recurvata*), *n*=16 (*Dioscorea elephantipes*), *n*=12 (*Gloriosa superba*), *n*=12 (*Arisaema tortuosum*), *n*=39 (*Acorus calamus*). White arrowheads indicate the graft junctions (**c**, **d**). Scale-bars represent 1 mm (**a**, **c**) or 200 μm (**b**, **d**).

Extended Data Fig. 8. Intra- and inter-specific graft combinations in Poaceae. a, Phylogenetic reconstruction of the twelve subfamilies comprising the Poaceae (grass family). Species grafted are shown in bold. **b**, Rates of fusion between different varieties of the same C_3 or C_4 photosynthetic cereal crop species. **c**, Rates of fusion between different C_3 cereal species.

Extended Data Fig. 9. Complementation of rice defective in strigolactone biosynthesis by grafting mutants onto wild type rootstocks. a, Position of the *carotenoid cleavage dioxygenase 8* (*OsCCD8*, Os01g0746400) gene in the rice strigolactone biosynthesis pathway. Red color indicates the homozygous mutant *ccd8/ccd8* allele (the d10 mutant[44]). **b**, Height of the tallest ligule (upper plot), and length of the longest leaf (lower plot) on each grafted plant

946 measured over time. Statistically significant differences for tallest ligule height and longest leaf
947 length were assessed by two-way repeated measures ANOVA among graft types over time.
948 Letters indicate significant ($P < 0.05$) groupings among graft types at each time point using
949 pairwise *t*-tests with adjusted *P*-values by the Bonferroni multiple testing correction method.
950 ns = not significant. Data are presented as mean ± s.d. n=8. **c**, Shoot phenotypes of initial grafts
951 (upper panel) and their offspring derived from self-pollination (lower panel) after 40 days of
952 growth in soil. **d**, Rates of reversion to a high tillering (mutant) phenotype in the offspring of
953 self-pollinated grafts between *ccd8* mutant (d10) and wild type (*O. sativa* var. Shiokari).
954 Although the mutant phenotype was rescued when grafted to a wild type root system, offspring
955 of the mutant scions from such grafts reverted to the mutant phenotype, as expected. Scale-
956 bars represent 10 cm (**c**).

957

958 **Extended Data Fig. 10. Grafting wheat to oat confers disease tolerance to take-all. a**, A
959 schematic used for screening wheat, oat, and inter-tribal grafts between wheat and oat for take-
960 all disease, caused by the soil borne pathogen *G. graminis* var. *tritici*. **b**, Representative images
961 of self-grafted oat, self-grafted wheat, and inter-tribal grafts between wheat and an oat.
962 Transverse sections of each graft junction are shown in the upper right corner of each panel
963 seven days after grafting. n=6. **c**, Representative images of grafted plants seven days after
964 grafting and immediately after inoculation with an agar plug containing *G. graminis* var. *tritici*
965 (n = 6). The plug was placed directly on top of the roots to ensure physical contact between the
966 pathogen and rootstock. **d**, Representative images of grafted plants three weeks after
967 inoculation. Panels show high magnification of graft junction (left), side view of the culture
968 containers (middle), and a view looking down into the containers (right). **e**, Non-inoculated
969 control grafts, with side view of culture containers (left) and view looking down into the
970 container (right). White arrowheads indicate the graft junction (**a**-**e**), and empty black

971 arrowheads indicate disease progression into the scion past the graft junction (**d**). Scale bars
972 represent approximately 1 mm (**b**, **d** left panels), 250 μm (**b** upper right panels), 1 cm (**c**, **d**
973 middle and right, and **e**).

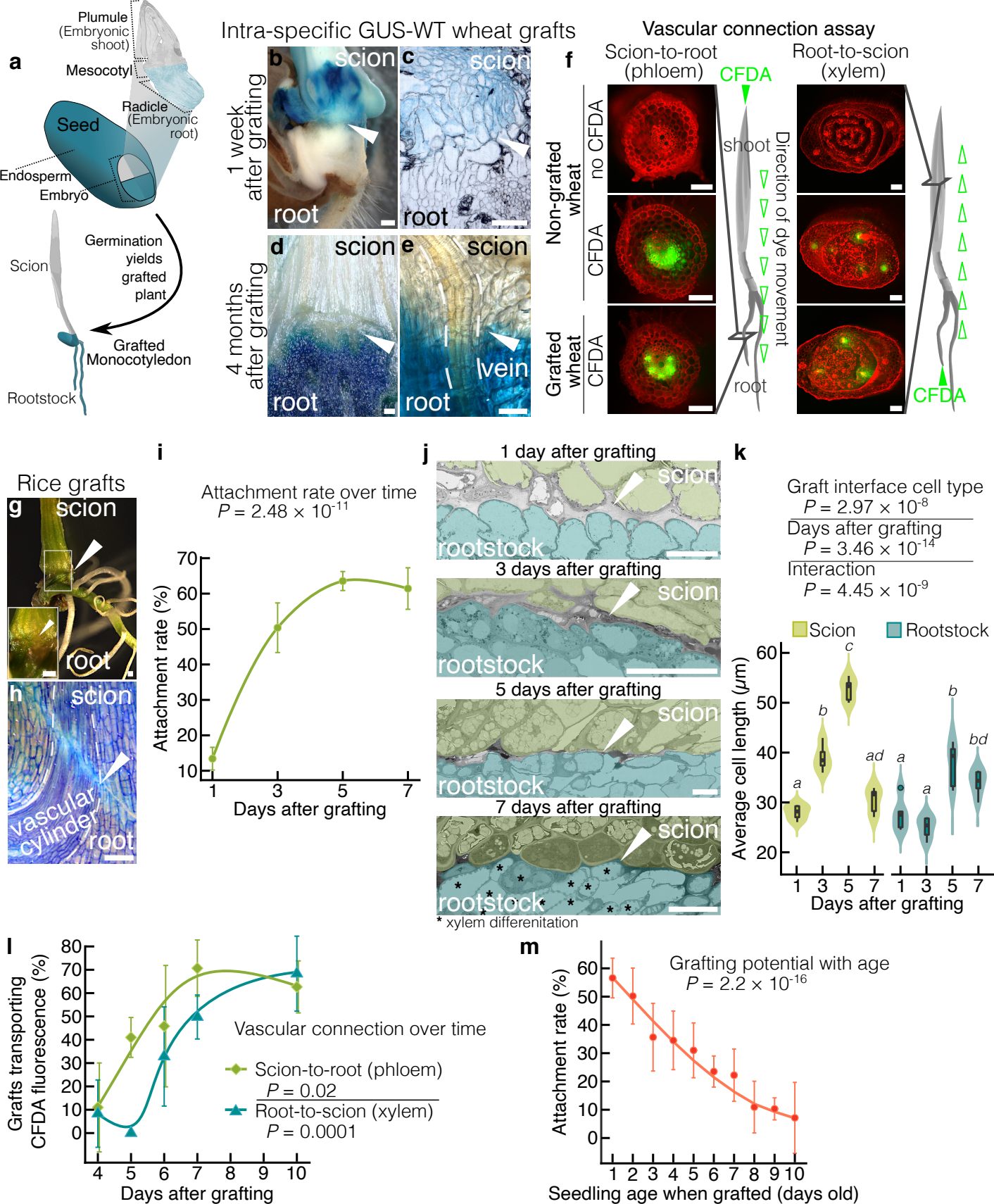
a
Plumule (Embryonic shoot)
Mesocotyl
Radicle (Embryonic root)
Seed
Endosperm
Embryo
Scion
Germination yields grafted plant
Grafted Monocotyledon
Rootstock
Intra-specific GUS-WT wheat grafts
1 week after grafting
4 months after grafting
b scion root
c scion root
d scion root
e scion vein root
f
Vascular connection assay
Scion-to-root (phloem)
Root-to-scion (xylem)
CFDA
Non-grafted wheat
no CFDA
CFDA
Grafted wheat
CFDA
shoot
root
Direction of dye movement
CFDA
Rice grafts
g scion root
h scion vascular cylinder root
i
Attachment rate over time
P = 2.48 × 10-11
Attachment rate (%)
Days after grafting
j
1 day after grafting
3 days after grafting
5 days after grafting
7 days after grafting
scion
rootstock
* xylem differenitation
k
Graft interface cell type
P = 2.97 × 10-8
Days after grafting
P = 3.46 × 10-14
Interaction
P = 4.45 × 10-9
Scion
Rootstock
Average cell length (μm)
Days after grafting
l
Grafts transporting CFDA fluorescence (%)
Vascular connection over time
Scion-to-root (phloem)
P = 0.02
Root-to-scion (xylem)
P = 0.0001
Days after grafting
m
Grafting potential with age
P = 2.2 × 10-16
Attachment rate (%)
Seedling age when grafted (days old)

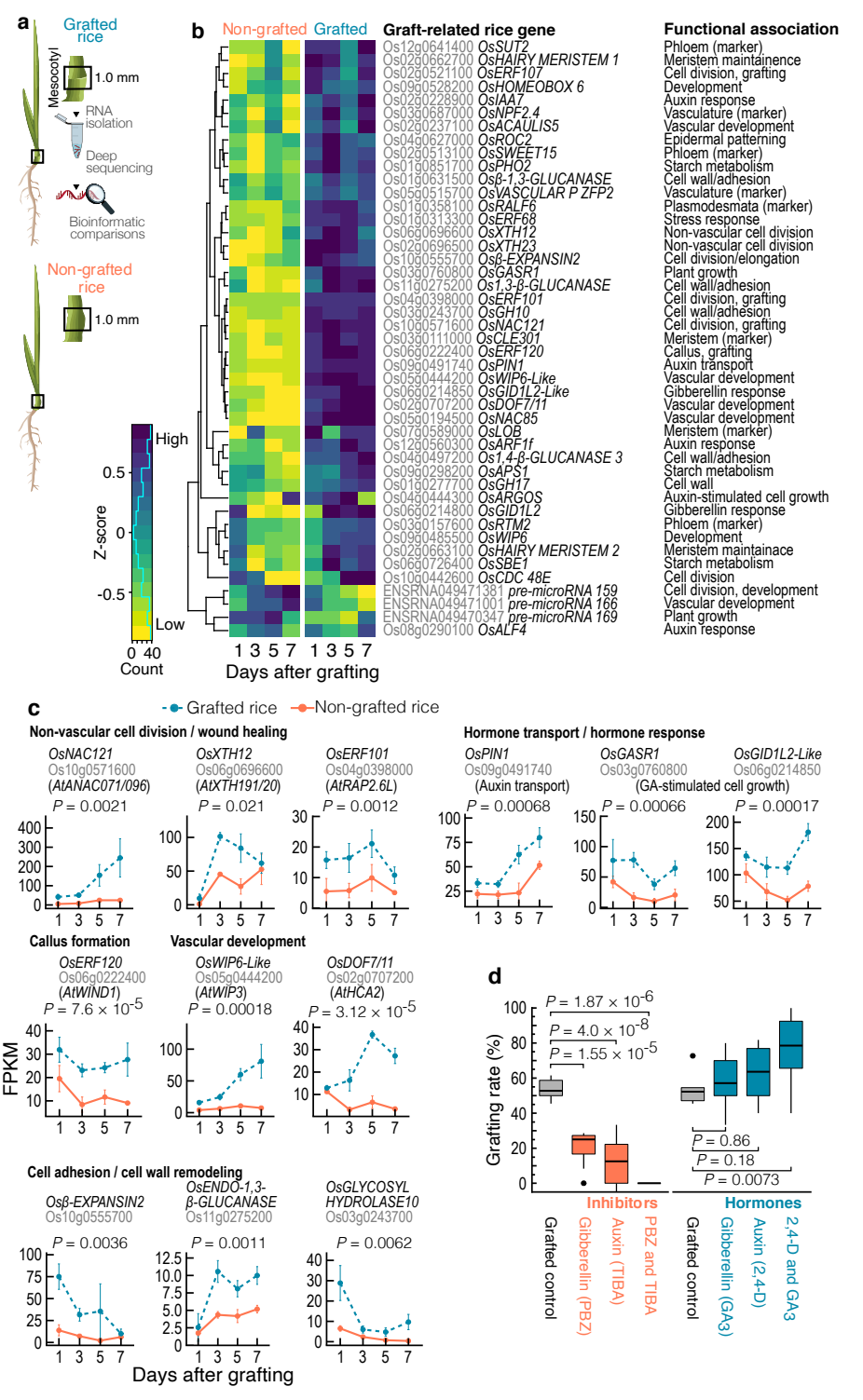
a
Grafted rice
Mesocotyl
1.0 mm
RNA isolation
Deep sequencing
Bioinformatic comparisons
Non-grafted rice
1.0 mm
High
Z-score
0.5
0
-0.5
Low
0 40
Count
b
Non-grafted
Grafted
Graft-related rice gene
Functional association
Os12g0641400 OsSUT2 Phloem (marker)
Os02g0662700 OsHAIRY MERISTEM 1 Meristem maintainence
Os02g0521100 OsERF107 Cell division, grafting
Os09g0528200 OsHOMEOBOX 6 Development
Os02g0228900 OsIAA7 Auxin response
Os03g0687000 OsNPF2.4 Vasculature (marker)
Os02g0237100 OsACAULIS5 Vascular development
Os04g0627000 OsROC2 Epidermal patterning
Os02g0513100 OsSWEET15 Phloem (marker)
Os01g0851700 OsPHO2 Starch metabolism
Os01g0631500 Osβ-1,3-GLUCANASE Cell wall/adhesion
Os05g0515700 OsVASCULAR P ZFP2 Vasculature (marker)
Os01g0358100 OsRALF6 Plasmodesmata (marker)
Os01g0313300 OsERF68 Stress response
Os06g0696600 OsXTH12 Non-vascular cell division
Os02g0696500 OsXTH23 Non-vascular cell division
Os10g0555700 Osβ-EXPANSIN2 Cell division/elongation
Os03g0760800 OsGASR1 Plant growth
Os11g0275200 Os1,3-β-GLUCANASE Cell wall/adhesion
Os04g0398000 OsERF101 Cell division, grafting
Os03g0243700 OsGH10 Cell wall/adhesion
Os10g0571600 OsNAC121 Cell division, grafting
Os03g0111000 OsCLE301 Meristem (marker)
Os06g0222400 OsERF120 Callus, grafting
Os09g0491740 OsPIN1 Auxin transport
Os05g0444200 OsWIP6-Like Vascular development
Os06g0214850 OsGID1L2-Like Gibberellin response
Os02g0707200 OsDOF7/11 Vascular development
Os05g0194500 OsNAC85 Vascular development
Os07g0589000 OsLOB Meristem (marker)
Os12g0560300 OsARF1f Auxin response
Os04g0497200 Os1,4-β-GLUCANASE 3 Cell wall/adhesion
Os09g0298200 OsAPS1 Starch metabolism
Os01g0277700 OsGH17 Cell wall
Os04g0444300 OsARGOS Auxin-stimulated cell growth
Os06g0214800 OsGID1L2 Gibberellin response
Os03g0157600 OsRTM2 Phloem (marker)
Os09g0485500 OsWIP6 Development
Os02g0663100 OsHAIRY MERISTEM 2 Meristem maintainace
Os06g0726400 OsSBE1 Starch metabolism
Os10g0442600 OsCDC 48E Cell division
ENSRNA049471381 pre-microRNA 159 Cell division, development
ENSRNA049471001 pre-microRNA 166 Vascular development
ENSRNA049470347 pre-microRNA 169 Plant growth
Os08g0290100 OsALF4 Auxin response
1 3 5 7 1 3 5 7
Days after grafting
c
Grafted rice
Non-grafted rice
Non-vascular cell division / wound healing
OsNAC121
Os10g0571600
(AtANAC071/096)
P = 0.0021
OsXTH12
Os06g0696600
(AtXTH191/20)
P = 0.021
OsERF101
Os04g0398000
(AtRAP2.6L)
P = 0.0012
Hormone transport / hormone response
OsPIN1
Os09g0491740
(Auxin transport)
P = 0.00068
OsGASR1
Os03g0760800
(GA-stimulated cell growth)
P = 0.00066
OsGID1L2-Like
Os06g0214850
P = 0.00017
Callus formation
OsERF120
Os06g0222400
(AtWIND1)
P = 7.6 × 10−5
Vascular development
OsWIP6-Like
Os05g0444200
(AtWIP3)
P = 0.00018
OsDOF7/11
Os02g0707200
(AtHCA2)
P = 3.12 × 10−5
FPKM
Cell adhesion / cell wall remodeling
Osβ-EXPANSIN2
Os10g0555700
P = 0.0036
OsENDO-1,3-β-GLUCANASE
Os11g0275200
P = 0.0011
OsGLYCOSYL HYDROLASE10
Os03g0243700
P = 0.0062
Days after grafting
d
Grafting rate (%)
P = 1.87 × 10−6
P = 4.0 × 10−8
P = 1.55 × 10−5
P = 0.86
P = 0.18
P = 0.0073
Inhibitors
Hormones
Grafted control
Gibberellin (PBZ)
Auxin (TIBA)
PBZ and TIBA
Grafted control
Gibberellin (GA3)
Auxin (2,4-D)
2,4-D and GA3

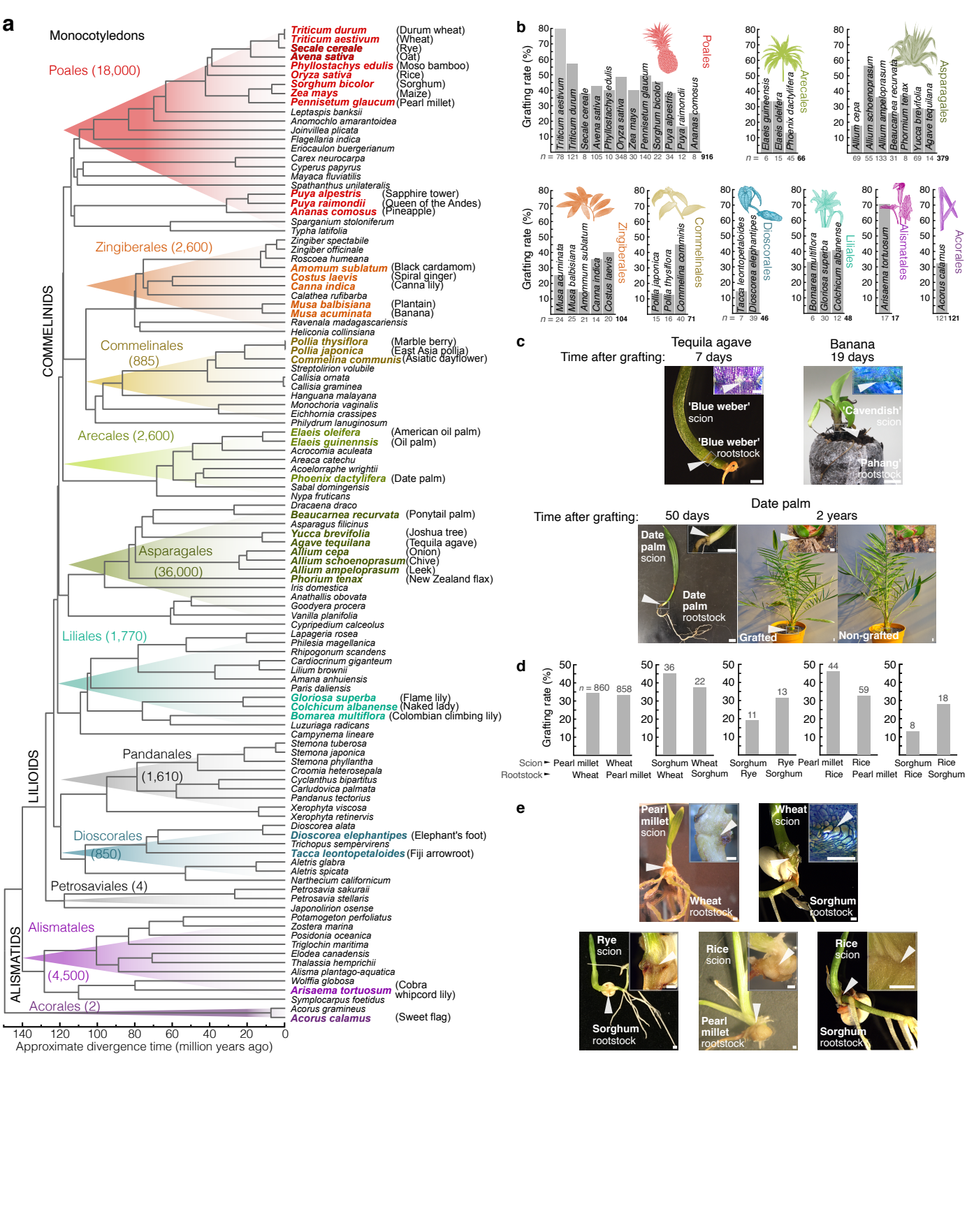
a
Monocotyledons
Poales (18,000)
Triticum durum (Durum wheat)
Triticum aestivum (Wheat)
Secale cereale (Rye)
Avena sativa (Oat)
Phyllostachys edulis (Moso bamboo)
Oryza sativa (Rice)
Sorghum bicolor (Sorghum)
Zea mays (Maize)
Pennisetum glaucum (Pearl millet)
Leptaspis banksii
Anomochlo amarantoidea
Joinvillea plicata
Flagellaria indica
Eriocaulon buergerianum
Carex neurocarpa
Cyperus papyrus
Mayaca fluviatilis
Spathanthus unilateralis
Puya alpestris (Sapphire tower)
Puya raimondii (Queen of the Andes)
Ananas comosus (Pineapple)
Sparganium stoloniferum
Typha latifolia
COMMELINIDS
Zingiberales (2,600)
Zingiber spectabile
Zingiber officinale
Roscoea humeana
Amomum sublatum (Black cardamom)
Costus laevis (Spiral ginger)
Canna indica (Canna lily)
Calathea rufibarba
Musa balbisiana (Plantain)
Musa acuminata (Banana)
Ravenala madagascariensis
Heliconia collinsiana
Commelinales (885)
Pollia thysiflora (Marble berry)
Pollia japonica (East Asia pollia)
Commelina communis (Asiatic dayflower)
Streptolirion volubile
Callisia ornata
Callisia graminea
Hanguana malayana
Monochoria vaginalis
Eichhornia crassipes
Philydrum lanuginosum
Arecales (2,600)
Elaeis oleifera (American oil palm)
Elaeis guineensis (Oil palm)
Acrocomia aculeata
Areaca catechu
Acoelorraphe wrightii
Phoenix dactylifera (Date palm)
Sabal domingensis
Nypa fruticans
Asparagales (36,000)
Dracaena draco
Beaucarnea recurvata (Ponytail palm)
Asparagus filicinus
Yucca brevifolia (Joshua tree)
Agave tequilana (Tequila agave)
Allium cepa (Onion)
Allium schoenoprasum (Chive)
Allium ampeloprasum (Leek)
Phorium tenax (New Zealand flax)
Iris domestica
Anathallis obovata
Goodyera procera
Vanilla planifolia
Cypripedium calceolus
Liliales (1,770)
Lapageria rosea
Philesia magellanica
Rhipogonum scandens
Cardiocrinum giganteum
Lilium brownii
Amana anhuiensis
Paris daliensis
Gloriosa superba (Flame lily)
Colchicum albanense (Naked lady)
Bomarea multiflora (Colombian climbing lily)
Luzuriaga radicans
Campynema lineare
LILIOIDS
Pandanales (1,610)
Stemona tuberosa
Stemona japonica
Stemona phyllantha
Croomia heterosepala
Cyclanthus bipartitus
Carludovica palmata
Pandanus tectorius
Xerophyta viscosa
Xerophyta retinervis
Dioscorea alata
Dioscorales (850)
Dioscorea elephantipes (Elephant's foot)
Trichopus sempervirens
Tacca leontopetaloides (Fiji arrowroot)
Aletris glabra
Aletris spicata
Petrosaviales (4)
Narthecium californicum
Petrosavia sakuraii
Petrosavia stellaris
Japonolirion osense
Potamogeton perfoliatus
Zostera marina
Alismatales (4,500)
Posidonia oceanica
Triglochin maritima
Elodea canadensis
Thalassia hemprichii
Alisma plantago-aquatica
Wolffia globosa
Arisaema tortuosum (Cobra whipcord lily)
ALISMATIDS
Acorales (2)
Symplocarpus foetidus
Acorus gramineus
Acorus calamus (Sweet flag)
140 120 100 80 60 40 20 0
Approximate divergence time (million years ago)
b
Grafting rate (%)
Poales
Triticum aestivum
Triticum durum
Secale cereale
Avena sativa
Phyllostachys edulis
Oryza sativa
Zea mays
Pennisetum glaucum
Sorghum bicolor
Puya alpestris
Puya raimondii
Ananas comosus
n = 78 121 8 105 10 348 30 140 22 34 12 8 916
Arecales
Elaeis guineensis
Elaeis oleifera
Phoenix dactylifera
n = 6 15 45 66
Asparagales
Allium cepa
Allium schoenoprasum
Allium ampeloprasum
Beaucarnea recurvata
Phormium tenax
Yucca brevifolia
Agave tequilana
69 55 133 31 8 69 14 379
Zingiberales
Musa acuminata
Musa balbisiana
Amomum sublatum
Canna indica
Costus laevis
n = 24 25 21 14 20 104
Commelinales
Pollia japonica
Pollia thysiflora
Commelina comminis
15 16 40 71
Dioscorales
Tacca leontopetaloides
Dioscorea elephantipes
n = 7 39 46
Liliales
Bomarea multiflora
Gloriosa superba
Colchicum albanense
6 30 12 48
Alismatales
Arisaema tortuosum
17 17
Acorales
Acorus calamus
121 121
c
Tequila agave
Time after grafting: 7 days
'Blue weber' scion
'Blue weber' rootstock
Banana
19 days
'Cavendish' scion
'Pahang' rootstock
Date palm
Time after grafting: 50 days
2 years
Date palm scion
Date palm rootstock
Grafted
Non-grafted
d
Grafting rate (%)
n = 860
858
36
22
11
13
44
59
8
18
Scion
Rootstock
Pearl millet
Wheat
Sorghum
Rye
Rice
e
Pearl millet scion
Wheat rootstock
Wheat scion
Sorghum rootstock
Rye scion
Sorghum rootstock
Rice scion
Pearl millet rootstock
Rice scion
Sorghum rootstock

a Strigolactone mutant complementation

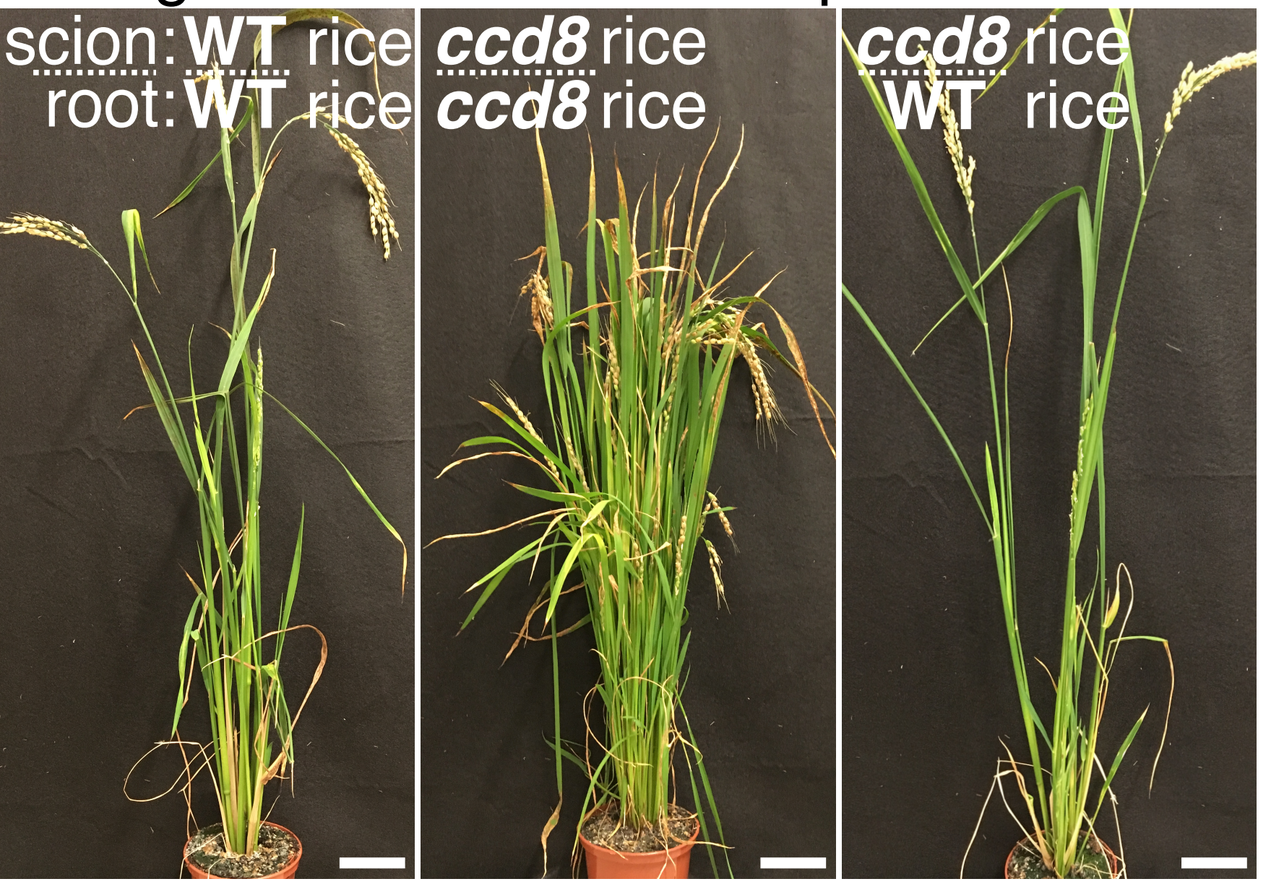

b

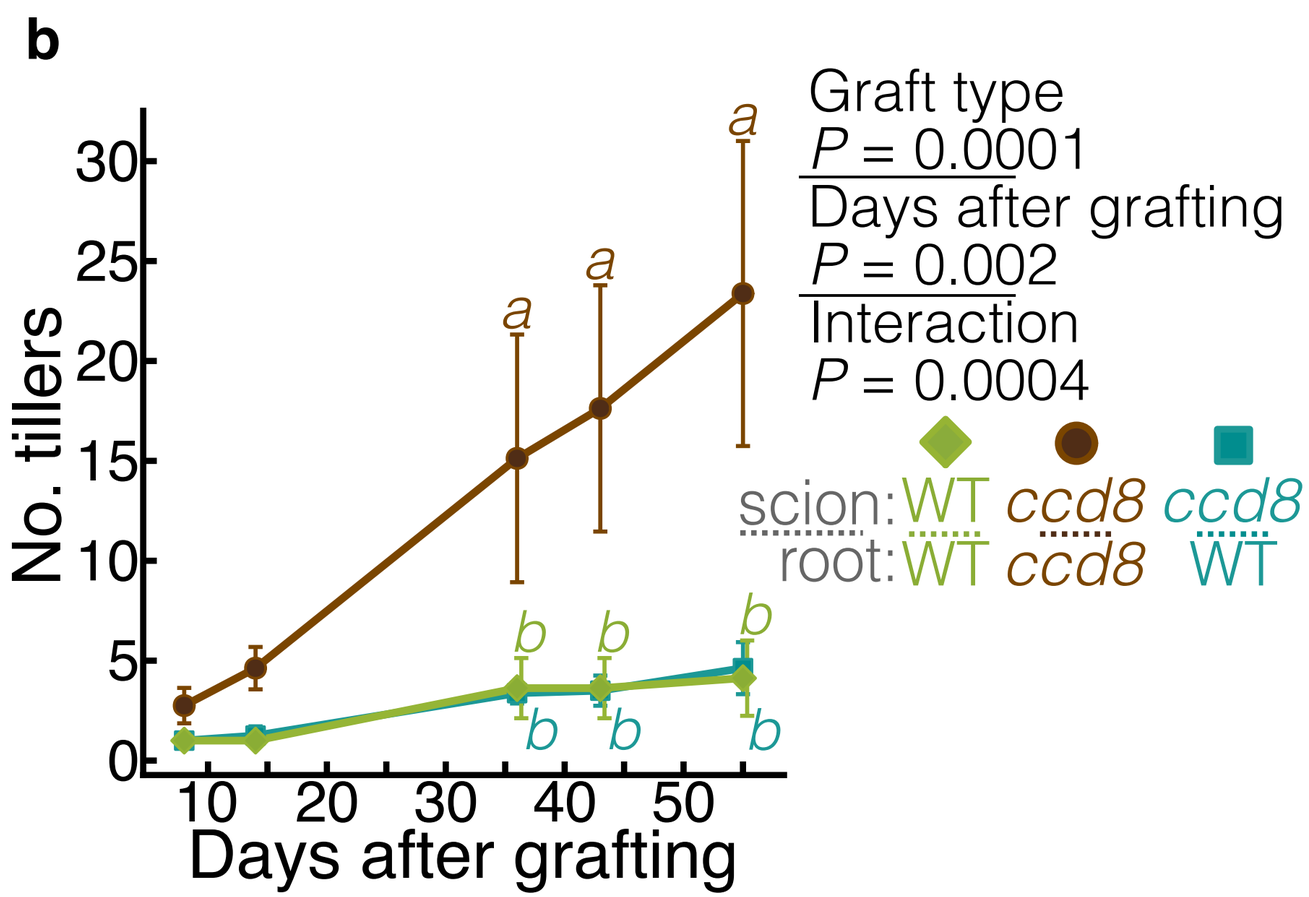

c Take-all disease tolerance

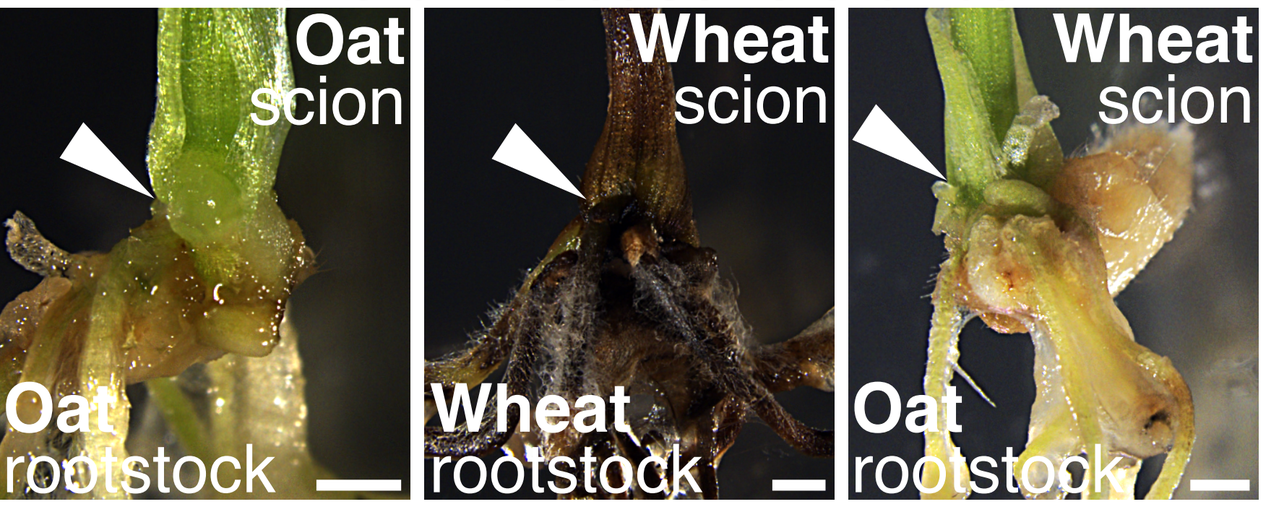

d

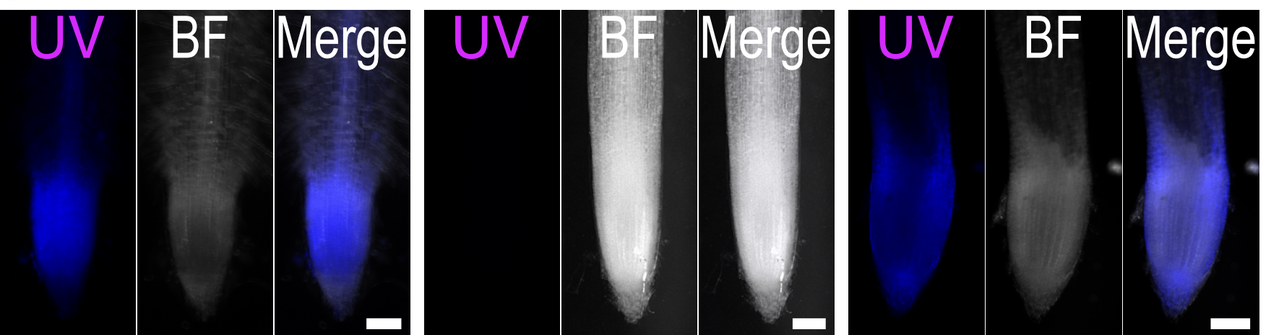

e

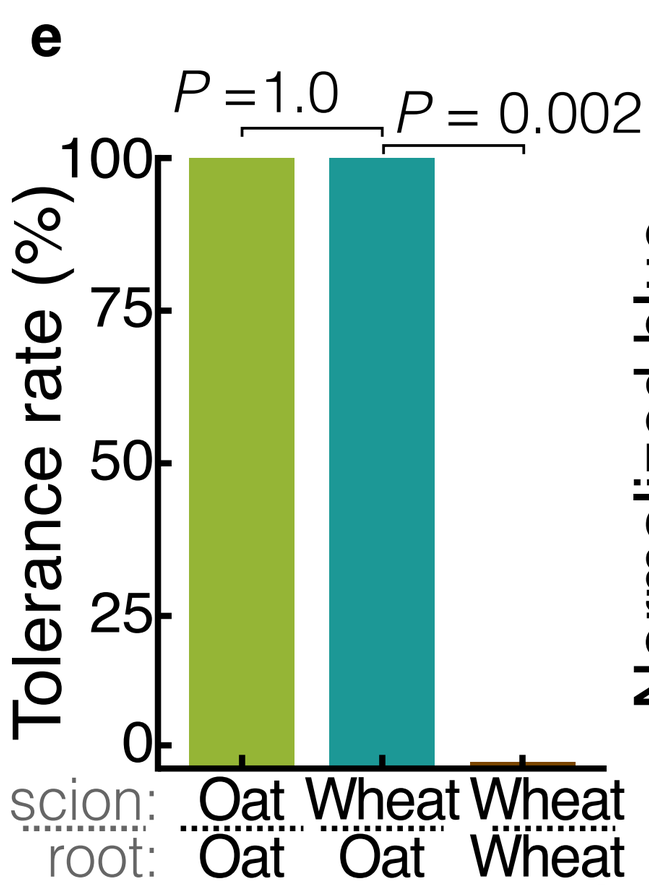

f